Mapping of the nucleolar proteome reveals spatiotemporal organization related to intrinsic protein disorder

Lovisa Stenström[1], Diana Mahdessian[1], Christian Gnann[1,2], Manuel D. Leonetti[2], Mathias Uhlén[1], Sara Cuylen-Häring[3], Peter J. Thul[1], Emma Lundberg[1,2,4*]

[1]Science for Life Laboratory, School of Engineering Sciences in Chemistry, Biotechnology and Health, KTH Royal Institute of Technology, SE-171 21 Stockholm, Sweden.
[2] Chan Zuckerberg Biohub, San Francisco, CA 94158.
[3] Cell Biology and Biophysics Unit, Structural and Computational Biology Unit, European Molecular Biology Laboratory, Heidelberg, Germany.
[4] Department of Genetics, Stanford University, Stanford, CA, USA.

[*]Correspondence to: emma.lundberg@scilifelab.se

Keywords: Nucleolus, perichromosomal layer, intrinsic protein disorder, Human Protein Atlas

Abstract

The nucleolus is essential for ribosome biogenesis, but also involved in many other cellular functions. We performed a systematic spatiotemporal dissection of the human nucleolar proteome using confocal microscopy. In total, 1318 nucleolar proteins were identified; 287 localized to fibrillar components, and 157 were enriched along the nucleoplasmic border, indicating a unique proteome composition in this phase-separated region. We identified 65 nucleolar proteins (36 unknown) to relocate to the chromosomal periphery during mitosis. Interestingly, we here observed a temporal partitioning into two phenotypes; early (prometaphase), or late (after metaphase) recruitment, suggesting phase specific functions. We further show that expression of MKI67 is critical for this temporal partitioning. We provide the first proteome-wide analysis of intrinsic protein disorder for an organelle, and show that nucleolar proteins in general, and mitotic chromosome proteins in particular, have significantly higher intrinsic disorder level compared to cytosolic proteins, indicating that the perichromosomal layer is liquid-like. In summary, this study provides a comprehensive and essential resource of spatiotemporal expression data for the nucleolar proteome as part of the Human Protein Atlas.

Introduction

One of the most prominent nuclear substructures is the nucleolus, the cellular site for ribosome synthesis and assembly. In addition to this key function the nucleoli comprise proteins shown to be involved in cell cycle regulation and cell stress responses (Visintin and Amon, 2000; Boisvert *et al.*, 2007). Nucleoli form around nucleolar organizing regions on the ribosomal DNA sites (rDNA). As opposed to membrane-bound organelles, nucleoli and other nuclear bodies lack enclosing membranes. This allows for highly dynamic cellular responses as these structures can change in size and protein composition when needed. The size and number of nucleoli changes throughout the cell cycle as they fuse together, a process recently suggested to be aided by interactions with the nucleoplasm (Caragine, Haley and Zidovska, 2019). The formation of these membrane-less, yet spatially distinct structures is a result of reversible liquid-liquid phase transitions similar to oil in water emulsions (Brangwynne *et al.*, 2009; Brangwynne, Mitchison and Hyman, 2011; Lin *et al.*, 2015). In interphase, the nucleolus is structurally partitioned into three droplet-like layers with different miscibility (Feric *et al.*, 2016). This separation facilitates a sequential production of ribosomes, from transcription of rDNA at the fibrillar center border (FC) followed by rRNA processing in the dense fibrillar component (DFC) and ribosome assembly in the granular component (GC). Phase separation is a dynamic process dependent on external factors such as pH, temperature, protein posttranslational modifications (PTMs) but most importantly protein composition and concentration. One common trait among proteins able to form liquid-like droplets has shown to be the presence of low complexity sequence domains (LCDs) and protein disorder. Intrinsically disordered proteins (IDPs) are characterized by being fully or partially unfolded, making them flexible in terms of interaction and has also been suggested as being a strong driver of phase separation (Li *et al.*, 2012; Berry *et al.*, 2015; Elbaum-Garfinkle *et al.*, 2015; Molliex *et al.*, 2015; Nott *et al.*, 2015). IDPs have shown to been central in various diseases such as cancer, cardiovascular diseases and Alzheimer's. Mutations in disordered regions can drastically change the

conformation of the protein and as many IDPs function as hub-proteins, altered protein function could initiate a loss-of-function cascade in the cell (Uversky, Oldfield and Dunker, 2008).

The inherent high density of the nucleoli enables its isolation and purification. Several studies using mass spectrometry-based proteomics have been focused toward identifying proteins residing in the nucleoli (Andersen *et al.*, 2002, 2005; Scherl *et al.*, 2002; Leung *et al.*, 2006). Together they assign a nucleolar localization to over 700 proteins. Another intriguing finding is that the nucleolar proteome seems highly dynamic rather than static and containing many types of proteins not only related to ribosome biogenesis, indicating that the nucleolar proteome may be larger than previously expected.

As of today, there has been no effort to spatiotemporally map the human nucleolar proteome and its sub-compartments throughout the cell cycle. When the nucleolus disassembles during mitosis most nucleolar proteins leak to the cytoplasm. However, a majority of the mitotic chromosomal mass is not chromatin but other proteins residing in the perichromosomal layer including at least 50 nucleolar proteins (Gautier, Dauphin-Villemant, *et al.*, 1992; Gautier, Masson, *et al.*, 1992; Gautier, Robert-Nicoud, *et al.*, 1992; Angelier *et al.*, 2005; Van Hooser, Yuh and Heald, 2005; Takata *et al.*, 2007; Ohta *et al.*, 2010; Booth *et al.*, 2016). One example is the proliferation marker MKI67, a highly disordered nucleolar protein shown to be important for chromosome segregation by acting as an emulsifying shield around the chromosomes in mitosis (Booth *et al.*, 2014; Cuylen *et al.*, 2016).

In this study we used an antibody-based microscopy approach optimized within the Human Protein Atlas (HPA) project (Uhlen *et al.*, 2010; Thul *et al.*, 2017) to generate such a spatiotemporal map of the human nucleolar proteome in interphase and mitosis. We present a resource containing localization data for 1,318 nucleolar proteins

including a refined spatial sublocalization to the fibrillar center and the nucleoli rim, accessible as part of the HPA database (www.proteinatlas.org). Additionally, we show evidence for 65 nucleolar proteins being recruited to the chromosomal periphery during mitosis. Based on this subcellular map we also performed the first systematic analysis of intrinsic protein disorder for the human nucleolar proteins and conclude that a majority of the proteins have long intrinsically disordered domains.

Results

A detailed spatial map of the nucleolar proteome

Despite the nucleolus being an intensively studied organelle, there is currently no resource offering a complete map of the human nucleolar proteome. To address this matter, we used an immunofluorescence (IF) and confocal microscopy workflow developed within the HPA Cell Atlas to systematically map all human nucleolar proteins (Thul *et al.*, 2017). Out of the 12,393 proteins currently mapped in the HPA Cell Atlas (proteinatlas.org), we identified 1,318 nucleolar proteins (7 % of the localized human proteome) of which 287 localized to the fibrillar center or dense fibrillar component (from now on collectively denoted as fibrillar center) and 1,031 to the whole nucleoli (Table S1). A schematic image of the tripartite nucleolar organization is shown in Fig. 1A while Fig. 1B-C highlight typical output images of proteins localizing to the different nucleolar subcompartments. UTP6, a protein thought to be involved in pre-18S ribosomal RNA based on its yeast homolog, is known to localize to nucleoli (Fig. 1B) (Dragon *et al.*, 2002). UBTF activates RNA polymerase I mediated transcription in the fibrillar center (Fig. 1C) (Kwon and Green, 1994). Functional enrichment analysis of the nucleolar proteome shows that the enriched Gene Ontology (GO) terms for biological process are well in line with the known functions of the nucleoli, for example ribosome biogenesis, rRNA processing and transcription (Table S2).

Most nucleolar proteins are multilocalizing

One of the advantages with image-based proteomics is the ability to study the *in situ* protein localization in single cells. This also applies to multilocalizing proteins, as they are easily detected even when the protein abundance in one compartment is much higher than in other organelles. As much as 87% of the nucleolar proteins are also detected in one or several other cellular compartments (n=1,145). Of those, around 50% are other locations within the nucleus. The most commonly shared localization is the nucleoplasm, cytosol or mitochondria. LEO1 is a nucleoplasmic protein part of the PAF1

complex involved in transcription but has no previous experimental evidence for a nucleolar localization (Rozenblatt-Rosen *et al.*, 2005; Zhao, Tong and Zhang, 2005). However, using both antibodies and a GFP-tagged cell line we detected LEO1 in the nucleoplasm and the fibrillar center (Fig. 1D, antibody staining in wild type cells Fig. S1). A protein association network of the shared proteomes between the nucleolus and cytosol shows a tightly connected cluster, indicating association to the same biological functions (Fig. S2). Given that the nucleoli synthesize and assemble ribosomes for export to the cytoplasm, multilocalizing nucleolar and cytosolic proteins could be involved in translation. The ribosomal protein cluster in the core of the network supports this. One such example is the ribosomal protein RPL13 (Fig. 1E, siRNA antibody validation Fig. S3). The high number of multilocalizing nucleolar proteins suggests a functional versatility of these proteins, likely not only relating to ribosome biogenesis.

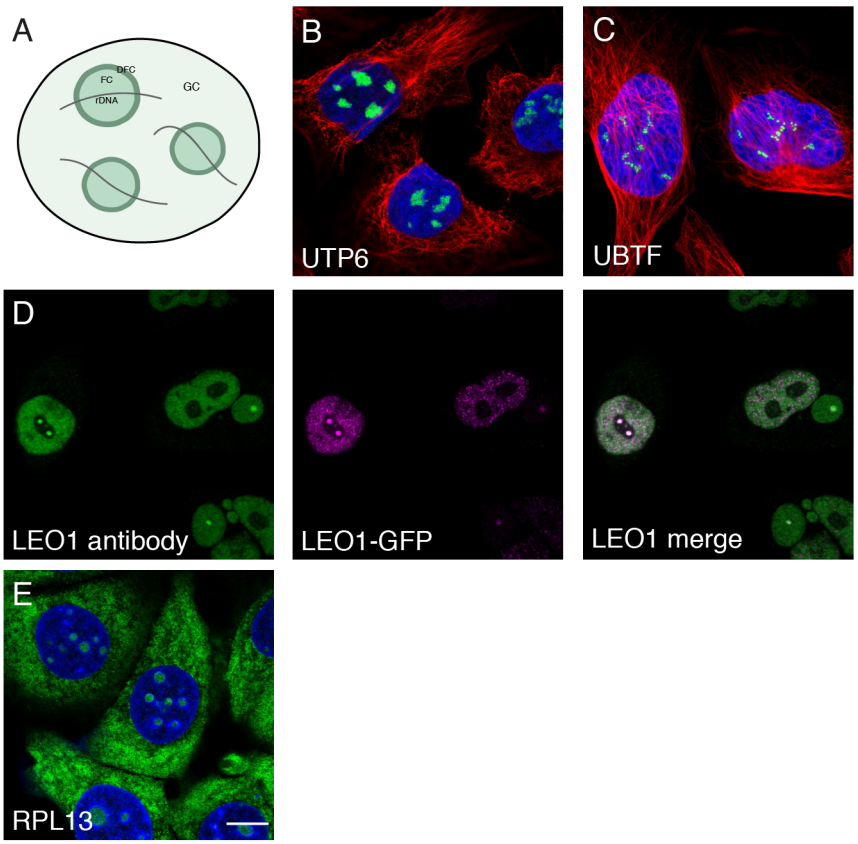

Figure 1 - A detailed spatial map of the nucleolar human proteome. Protein of interest is shown in green, nuclear marker DAPI in blue and the reference marker of microtubules in red. The antibody used is stated in parenthesis. Scale bar 10 µm. A) Schematic overview of the nucleolus and its substructures. Fibrillar center (FC), dense fibrillar component (DFC) and granular component (GC). B) UTP6 in U-2 OS cells exemplifies proteins localizing to the whole nucleoli (HPA025936). C) Fibrillar center localization shown by a UBTF IF staining in U-2 OS cells (HPA006385). D) Dual localization of LEO1 to both the fibrillar center and nucleoplasm in GFP-tagged HeLa cells (magenta), also supported by IF antibody staining using HPA040741 (green). E) The multilocalizing ribosomal protein RPL13 detected in the nucleoli, cytosol and ER in MCF-7 cells (HPA051702).

The nucleolar proteome is larger than previously thought

Based on our data the nucleolus comprises around 7 % of the human proteins, which is a higher number than previously proposed using mass spectrometry based methods (Andersen *et al.*, 2002, 2005; Scherl *et al.*, 2002; Leung *et al.*, 2006)**.** To demonstrate the reliability of our data we introduced a scoring system for each protein localization; enhanced, supported, approved or uncertain. The score depends on available additional validation methods such as siRNA knock down, but also similarity in immunostaining patterns between independent antibodies or consistency with available experimental localization data in the UniProtKB/Swiss-Prot database (The UniProt Consortium, 2019). The requirements for each score are described in detail in the Materials and Methods section and the distribution of localization scores for the nucleolar proteins is shown in Fig. S4.

When comparing the nucleolar dataset to the proteins with an experimentally verified nucleolar annotation in GO, the overlap is poor (Fig. S5). At least 700 proteins have been reported as nucleolar in literature (Andersen *et al.*, 2002, 2005; Scherl *et al.*, 2002; Leung *et al.*, 2006), while currently only 264 nucleolar proteins are incorporated into

GO. This poor coverage highlights the need for an updated resource detailing the nucleolar proteome. In our dataset, we have identified several previously uncharacterized nucleolar proteins. For instance the nucleolar protein KRI1 (Fig. 2A and Fig. S6 for independent antibody staining and siRNA antibody validation) that might be required for ribosome biogenesis (Sasaki, Toh-e and Kikuchi, 2000; Huh *et al.*, 2003) and the fibrillar center protein ZNRD1 (Fig. 2B and Fig. S6 for independent antibody staining), a component of the RNA polymerase I complex, which is involved in rDNA transcription (Mullem *et al.*, 2002; Huh *et al.*, 2003) based on data from their yeast homologs. Both these proteins only have previous experimental localization data in yeast cells and we can confirm a nucleolar localization also in human cells. The previously uncharacterized proteins FOXL2NB and FAM71E1 was localized to the fibrillar center (Fig. 2C-D, Fig. S6 for FOXL2NB independent antibody staining) as well as LRRC23, ZNF853 and METTL5 (Fig. 2E-G and Fig. S6 for LRRC23 independent antibody staining) being experimentally shown to localize to the nucleoli.

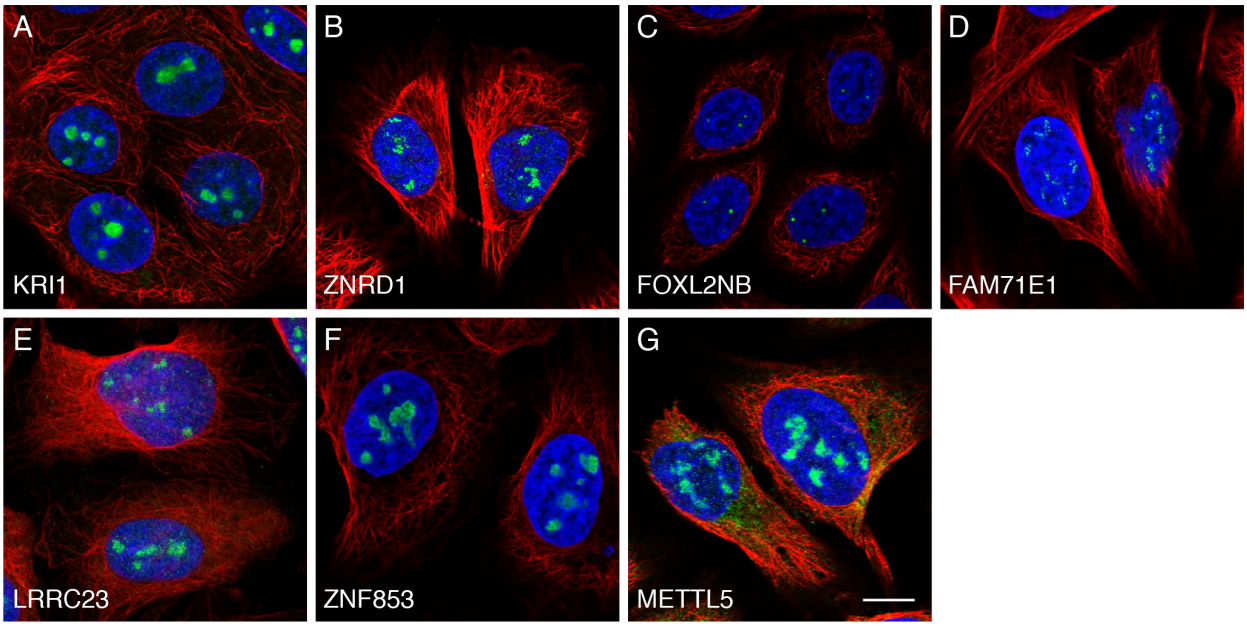

Figure 2 - Previously unknown nucleolar proteins. Protein of interest is shown in green, nuclear marker DAPI in blue and the reference marker of microtubules in red.

The antibody used is stated in parenthesis. Scale bar 10 µm. A) KRI1 localized to the nucleoli in MCF-7 cells (HPA043574). B) ZNRD1 localized to the fibrillar center in U-2 OS cells (HPA055074). C) FOXL2NB localized to the fibrillar center in SiHa cells (HPA061017). D) FAM71E1 localized to the fibrillar in U-2 OS cells (HPA048111). E) LRRC23 localized to the nucleoli in U-2 OS cells. F) ZNF853 localized to the nucleoli in U-2 OS cells (HPA057533). G) METTL5 localized to the nucleoli in U-2 OS cells (HPA038223).

The nucleoli rim staining could represent a nucleolar partition with a distinct proteomic profile

Despite the lack of an enclosing membrane, 157 of the nucleolar proteins show a characteristic rim-like staining pattern in at least one cell line, hereby denoted as nucleoli rim (Table S1). Two such examples is MKI67 that localizes to the nucleoli rim using three independent antibodies in all cell lines stained (Fig. 3A and Fig. S7) and GNL3 (Fig. 3B). The rim localization pattern has previously been proposed to be an antibody artifact related to abundant proteins sterically hindering the antibody to penetrate the whole nucleoli resulting in a staining gradient similar to the rim localization (Sheval *et al.*, 2005; Svistunova *et al.*, 2012). To investigate this we compared the mRNA expression of the rim proteins to the non-rim nucleolar proteins in the U-2 OS cell line. Despite that there is no perfect correlation between mRNA and protein level in cells, this could still be an indication if the nucleoli rim proteins are more highly expressed in general compared to the other nucleolar proteins. However, no significant difference in abundance could be seen on a transcriptional level (Fig. S8). This implies that protein abundance is not the only factor driving the rim localization. To further confirm that the rim staining is not an antibody artifact we created two cell lines expressing mNeonGreen-tagged MKI67 and GNL3 at endogenous levels, tagged at the N-terminus and C-terminus respectively. Live cell imaging revealed a dimmer, but still visible, rim localization for MKI67 also in the tagged cell line that was further enhanced upon PFA fixation (Fig. 3C-D). The rim localization could also be confirmed for GNL3 in

the tagged cells (Fig. 3E). Since the rim localization also is visible in the tagged cell lines, we conclude that proteins localizing to the nucleolar rim cannot only be considered an antibody artifact but potentially also a sign of a nucleolar partition with a distinct proteomic profile. The occurrence of this staining pattern seems to be more complex and that these proteins have other common molecular or functional features giving rise to this organization.

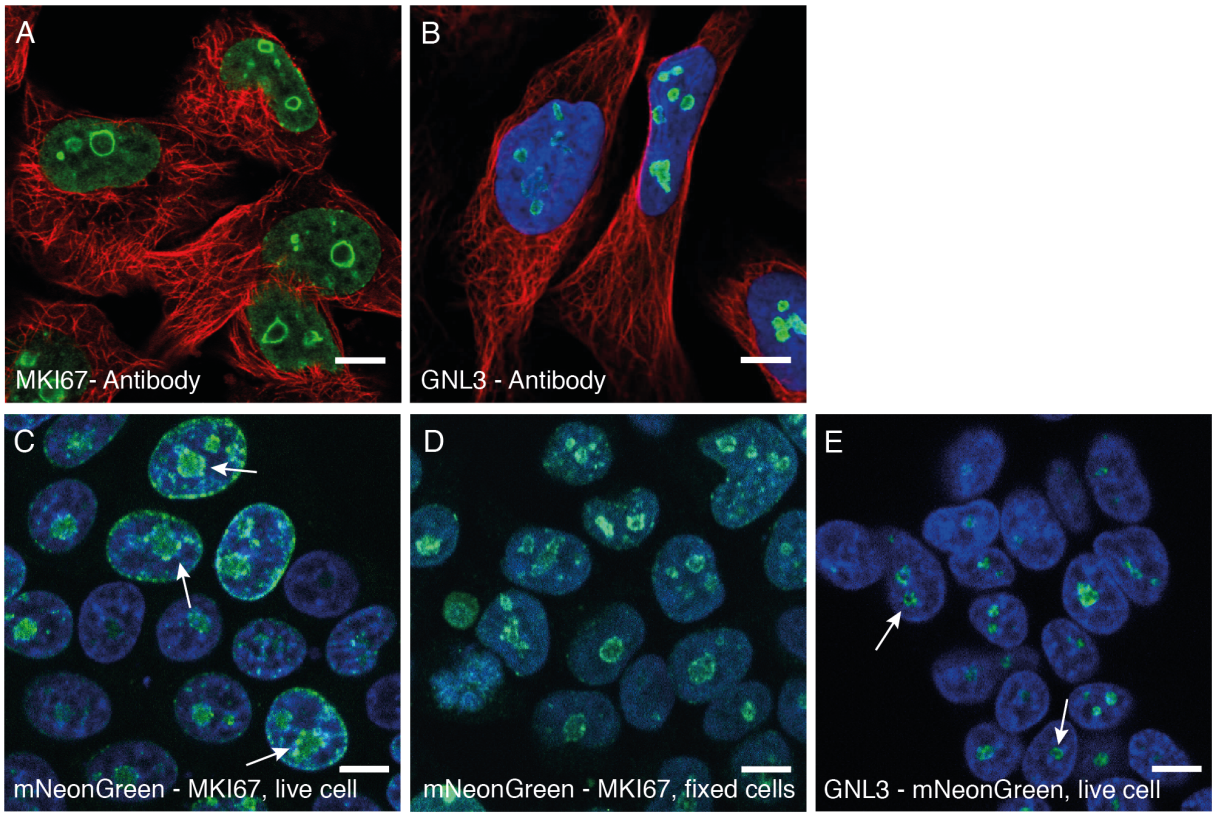

Figure 3 - The nucleoli rim localization. Protein of interest is shown in green, nuclear marker DAPI/Hoechst in blue and microtubules reference marker in red. The antibody used is stated in parenthesis. Scale bar 10 µm. A) IF staining of MKI67 shows localization to nucleoli rim in U-251 cells (CAB000058). B) IF staining of GNL3 shows localization to nucleoli rim in U-2 OS cells (HPA036743). C) HEK 293 cells expressing endogenous levels of N-terminus tagged MKI67 also show a faint nucleoli rim localization, although still visible. White arrows indicate cells were the rim could be seen. D) Fixed HEK 293 cells expressing tagged MKI67 shows even clearer nucleoli rim

localization. E) HEK 293 cells expressing endogenous levels of C-terminus tagged GNL3 also nucleoli rim localization. White arrows indicate cells were the rim could be seen.

Nucleolar proteins recruited to mitotic chromosomes

As the cell enters mitosis the nucleoli are disassembled to enable separation of the chromosomes. Most nucleolar proteins leak to the cytoplasm while at least 50 nucleolar proteins have been shown to instead adhere to the periphery of the chromosomes (Gautier, Dauphin-Villemant, *et al.*, 1992; Gautier, Masson, *et al.*, 1992; Gautier, Robert-Nicoud, *et al.*, 1992; Angelier *et al.*, 2005; Van Hooser, Yuh and Heald, 2005; Takata *et al.*, 2007; Ohta *et al.*, 2010). To better understand the nucleolar dynamics during mitosis we performed a single-cell spatial characterization of nucleolar proteins during cell division. MKI67 is as previously mentioned one of the more prominent perichromosomal constituents. Thus, we generated a list of 150 targets with connections to MKI67 or its interacting protein NIFK in a protein-protein association network or showing similar staining pattern in interphase as MKI67 (i.e. nucleoli rim) (Table S3). A mitotic shake off protocol was used to enrich mitotic cells from an asynchronous cell population. 85 nucleolar proteins could not be detected on the chromosomal periphery during cell division as exemplified by the ribosomal protein RPS19BP1 (Fig. S9). Apart from MKI67 (Fig. 4A) 65 proteins relocated to the chromosomal periphery of which 36 have, to our knowledge, no experimental data for being localized to chromosomes during cell division. Here exemplified by the proteins NOC2L, EMG1, BMS1, BRIX1 and RSL1D1 (Fig. 4B-F, Fig. S10 for independent antibody stainings of NOC2L and BMS1). 7 proteins were previously detected in chicken cells and we provide the first experimental evidence for a chromosomal localization in human cells (Ohta *et al.*, 2010). For the remaining 22 proteins we confirmed their previously stated localization to the condensed mitotic chromosomes (Gerdes *et al.*, 1984; Weisenberger and Scheer, 1995; Westendorf *et al.*, 1998; Magoulas *et al.*, 1998; Olson, Dundr and Szebeni, 2000; Lerch-

Gaggl *et al.*, 2002; Angelier *et al.*, 2005; Takata *et al.*, 2007; Amin *et al.*, 2008; Gambe *et al.*, 2009; Hirano *et al.*, 2009; Hirai *et al.*, 2013; Booth *et al.*, 2014) (Table S3). A highly interesting observation is that a large fraction of the nucleoli rim proteins also relocate to the perichromosomal layer during mitosis (at least 30 % of all rim proteins). Assuming that the probability of a rim and non-rim protein localizing to mitotic chromosomes is equal and that the fraction of rim and non-rim proteins should be the same between the mitotic chromosome and the cytoplasmic leakage groups (73 rim out of 150 proteins, 49 %), the actual distribution of rim proteins being relocated to mitotic chromosomes is significantly higher (49 out of 65 mitotic chromosome proteins, 75 %. $p = 1.6 \times 10^{-5}$, using a Binomial test).

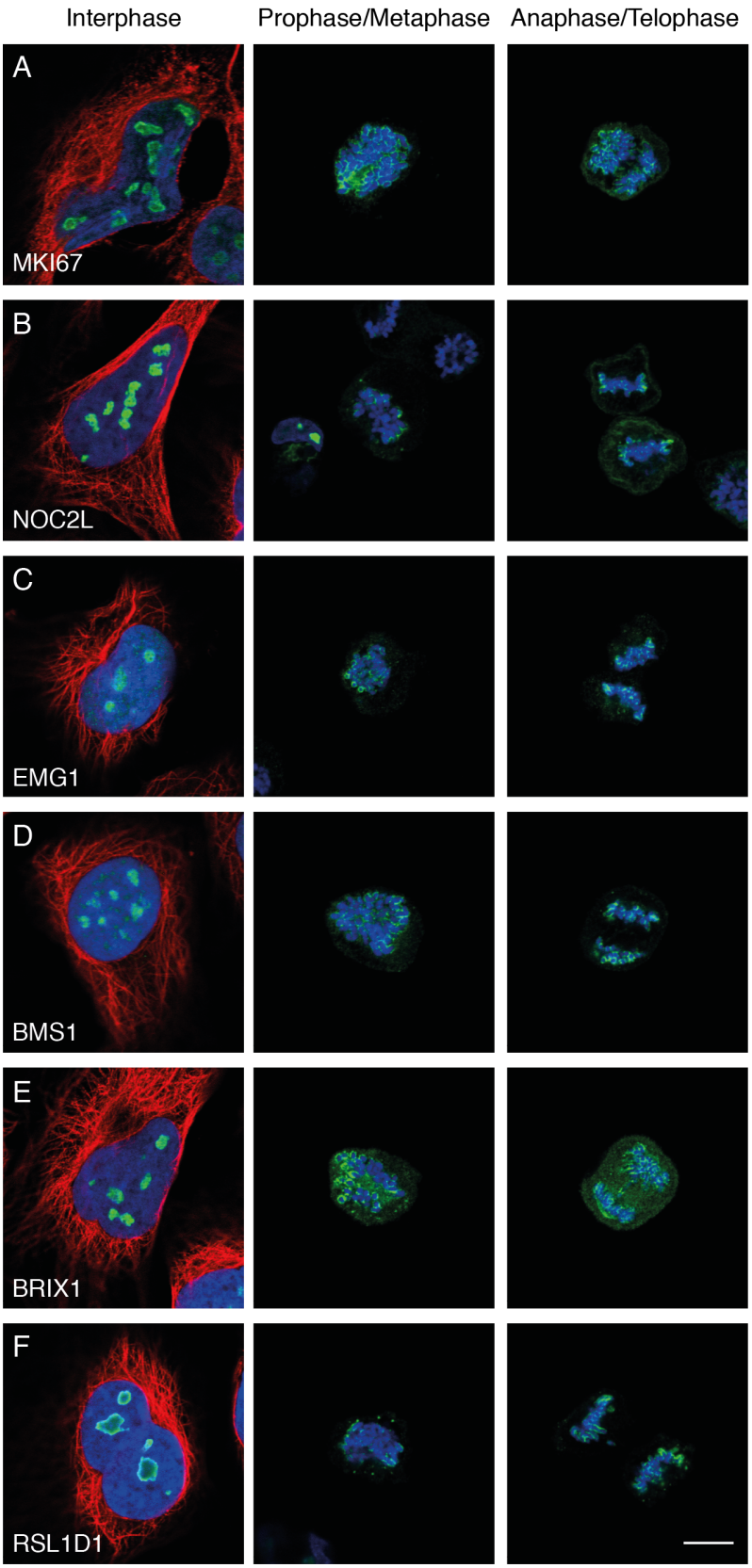

Figure 4 - Nucleolar proteins recruited to mitotic chromosomes. Protein of interest is shown in green, microtubules in red and DAPI in blue. Images of interphase cells were acquired from a different experiment and staining intensities cannot be compared between interphase and mitotic cells. Scale bar 10 µm. A) MKI67. B) NOC2L. C) EMG1. D) BMS1. E) BRIX1. F) RSL1D1.

Mitotic chromosome proteins are generally more disordered than other nucleolar proteins

Intrinsic protein disorder is a known key property for the formation of membrane-less organelles, such as the nucleolus (Elbaum-Garfinkle *et al.*, 2015; Molliex *et al.*, 2015; Nott *et al.*, 2015). To investigate this further we estimated the fraction of disordered residues among the nucleolar and mitotic chromosome proteins using the protein disorder prediction tool IUPred2A (Bálint, Gábor and Dosztányi, 2018). We then used the obtained disorder fractions to compare the nucleolar and mitotic chromosome proteins with the cytosolic proteins as defined in the HPA Cell Atlas (v19). The nucleolar proteins show a significantly higher fraction of disordered residues per protein with a median of 20 % compared to 14 % for the cytosolic proteins ($p_{adj} < 1x10^{-4}$ using Kruskal Wallis test followed by Dunn's test with Bonferroni correction). These numbers are similar to what previously have been shown for the mouse proteome where the authors conclude that the median disorder content for nucleolar proteins is 22 % and for non-nuclear proteins 12 % (Meng *et al.*, 2016). This supports the hypothesis of IDPs enriching in membrane-less structures where their phase-separation ability is needed to keep the structural integrity. Interestingly, the mitotic chromosome proteins are disordered to an even larger extent, median 36 % ($p_{adj} < 1x10^{-4}$ compared to both cytosolic proteins and to the nucleolar proteins) (Fig. 5A). Also the nucleoli rim proteins have a slightly higher disorder level than the other nucleolar proteins ($p_{adj} = 4x10^{-4}$). The number of proteins having at least one consecutive domain of more than 30 disordered residues, commonly considered as a functional domain, the same trend for the different

proteomes can be observed (Fig. 5B). More than 81 % of the proteins localizing to mitotic chromosomes have at least one disordered domain longer than 30 residues. Among the top five disordered mitotic chromosome proteins are the already known constituents of the perichromosomal layer CCDC86 (Ohta *et al.*, 2010) (known from chicken homolog data, Fig. 5C), CCDC137 (Ohta *et al.*, 2010; Booth *et al.*, 2014) and MKI67 (Gerdes *et al.*, 1984; Booth *et al.*, 2014; Cuylen *et al.*, 2016) but also the previously not described member of the perichromosomal layer, RRP15 (Fig. 5D). A study shows that RRP15 is central for rRNA transcription and biogenesis. The authors further present evidence of it being a checkpoint protein as perturbations of RRP15 induce nucleolar stress triggering cell cycle arrest (Dong *et al.*, 2017). Among the other highly disordered proteins is the uncharacterized protein PRR19, where we show experimental data for it being nucleolar in interphase and localized to the chromosomes during mitosis (Fig. 5E). We conclude that a majority of nucleolar mitotic chromosome proteins have at least one intrinsically disordered domain and that the fraction of disordered residues among nucleolar proteins is significantly higher compared to the average protein.

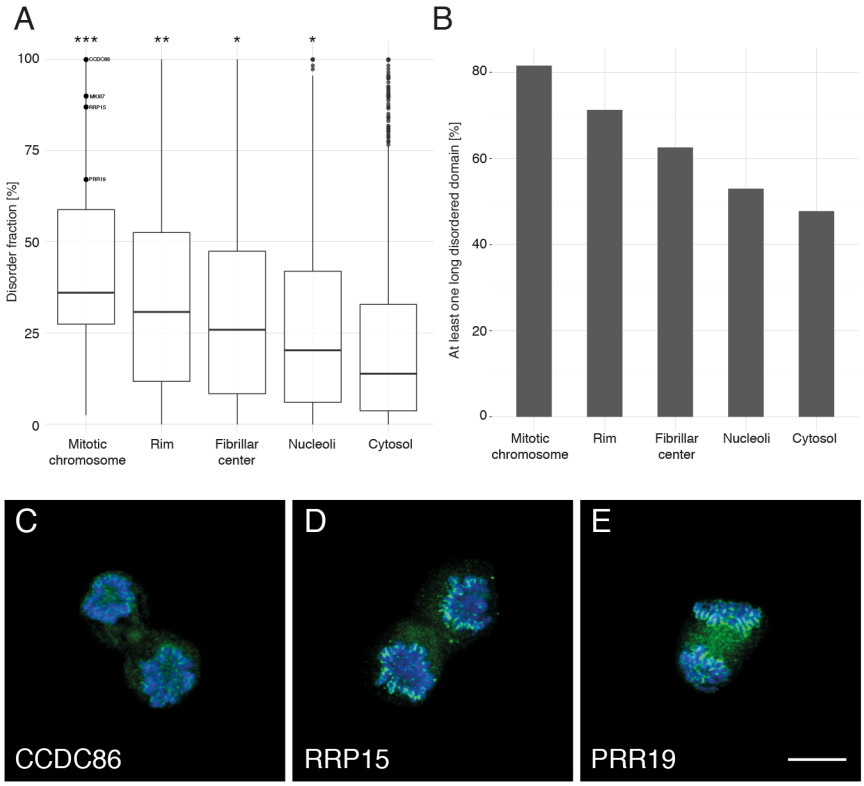

Figure 5 - Intrinsic disorder level for mitotic chromosome and nucleolar proteins as predicted by IUPRED2A. A) The fraction of disordered residues per protein for the nucleolar proteins is significantly higher (*, $p_{adj} < 1x10^{-4}$, Dunn's test with Bonferroni correction) compared to the cytosolic proteome as defined in the HPA Cell Atlas. Additionally, the disorder levels for the nucleoli rim proteins (**, $p_{adj} = 4x10^{-4}$) and the mitotic chromosome proteins (***, $p_{adj} < 1x10^{-4}$) are significantly higher compared to the other nucleolar proteins. B) Fraction of proteins having at least one functional disordered domain (>30 consecutive amino acids) for the mitotic chromosome dataset compared to the cytosolic proteome. More than 81 % of the mitotic chromosome proteins have at least one long disordered domain. C-E) Immunofluorescent stainings of previously uncharacterized mitotic chromosome proteins predicted to be highly disordered. Protein of interest shown in green and DAPI in blue. Scale bar 10 µm. C) CCDC86, 100% predicted disorder level. D) RRP15, 87% predicted disorder level. E) PRR19, 67% predicted disorder level.

Half of the mitotic chromosome proteins are essential for cell proliferation

Proteins being localized to the chromosomal surface during mitosis are expected to have a function important for cellular proliferation. To confirm this we examined the essential genes across different cancer cell lines in the Achilles dataset (Meyers *et al.*, 2017). It revealed that 34 of the mitotic chromosome genes are labeled as pan-dependent (Table S3), meaning that they have been ranked as the top most depleting genes in at least 90% of the cell lines screened. This is a significantly larger fraction relative all human genes but also compared to the whole nucleolar dataset (Pearson's Chi Squared test, p-value $2.2x10^{-16}$ and $5.3x10^{-10}$ respectively). When investigating the fraction of unfavorable marker genes predicted by the HPA Pathology Atlas, i.e. genes where a high expression had a negative association with patient survival ($p < 0.001$), the mitotic chromosome genes are significantly more prevalent ($n = 44$). Both compared to all detected genes and the nucleolar genes not localizing to mitotic chromosomes ($p = 3.0x10^{-8}$ and $p = 5.4x10^{-4}$ respectively). In total, 28 mitotic chromosome genes could be classified as both essential and unfavorable (Table S3). For instance, BYSL which is required for ribosome processing (Miyoshi *et al.*, 2007). It is labeled as pan dependent and its expression is predicted to be unfavorable in liver and renal cancer. DNTTIP2 is known to regulate the transcriptional activity in the nucleolus (Koiwai *et al.*, 2011). We additionally localized it to human mitotic chromosomes during cell division as it only has been detected on chicken chromosomes earlier (Ohta *et al.*, 2010) (Fig. S11). Similarly to BYSL it is pan dependent and its expression is unfavorable in both liver and renal cancer. CCDC137 is an unknown nucleolar protein but have previously been detected on chicken and human chromosomes (Ohta *et al.*, 2010; Booth *et al.*, 2014) (Fig. S11). Its function is unknown but is most likely important during cell division as being classified as both pan dependent and associated with poorer survival in renal, liver and lung cancer. We conclude that half of the mitotic chromosome genes are crucial for cell proliferation of cancer cells. However some proteins, for example MKI67, are not denoted as pan-dependent genes despite being known to perform essential functions during cell division. This highlights the advanced protein buffering capacity in the cell

but also that half of the mitotic chromosomal proteins in our dataset are needed for maintaining the proliferative ability.

Two expression phenotypes among mitotic chromosome proteins revealed

The large-scale studies done on the proteomic composition of the perichromosomal layer have been based on isolated chromosomes from a bulk of cells using mass spectrometry and hence been lacking a temporal dimension. By using IF we show that the recruitment of nucleolar proteins onto mitotic chromosomes can be stratified into two expression phenotypes, early (n = 45) and late recruitment (n = 20) (Table S3). MKI67 (Fig. 6A) highlights the early recruitment during prometaphase where an even staining intensity is kept throughout all mitotic phases**.** As opposed to this the late recruited proteins, exemplified by NOL12, TIGD1, BYSL, ACTL6B and ZNF202, consistently occurs after metaphase suggesting a phase specific function during mitosis (Fig. 6B-F, Fig. S10 for independent antibody staining of BYSL). ACTL6B has been detected on mitotic chromosomes in chicken cells (Ohta *et al.*, 2010) while the other highlighted proteins are previously unknown constituents of the chromosomal periphery. In total, we show experimental evidence for temporal partitioning of 65 nucleolar proteins at the surface of mitotic chromosomes, with 20 proteins having a later onset in terms of their chromosomal recruitment (Fig. S12).

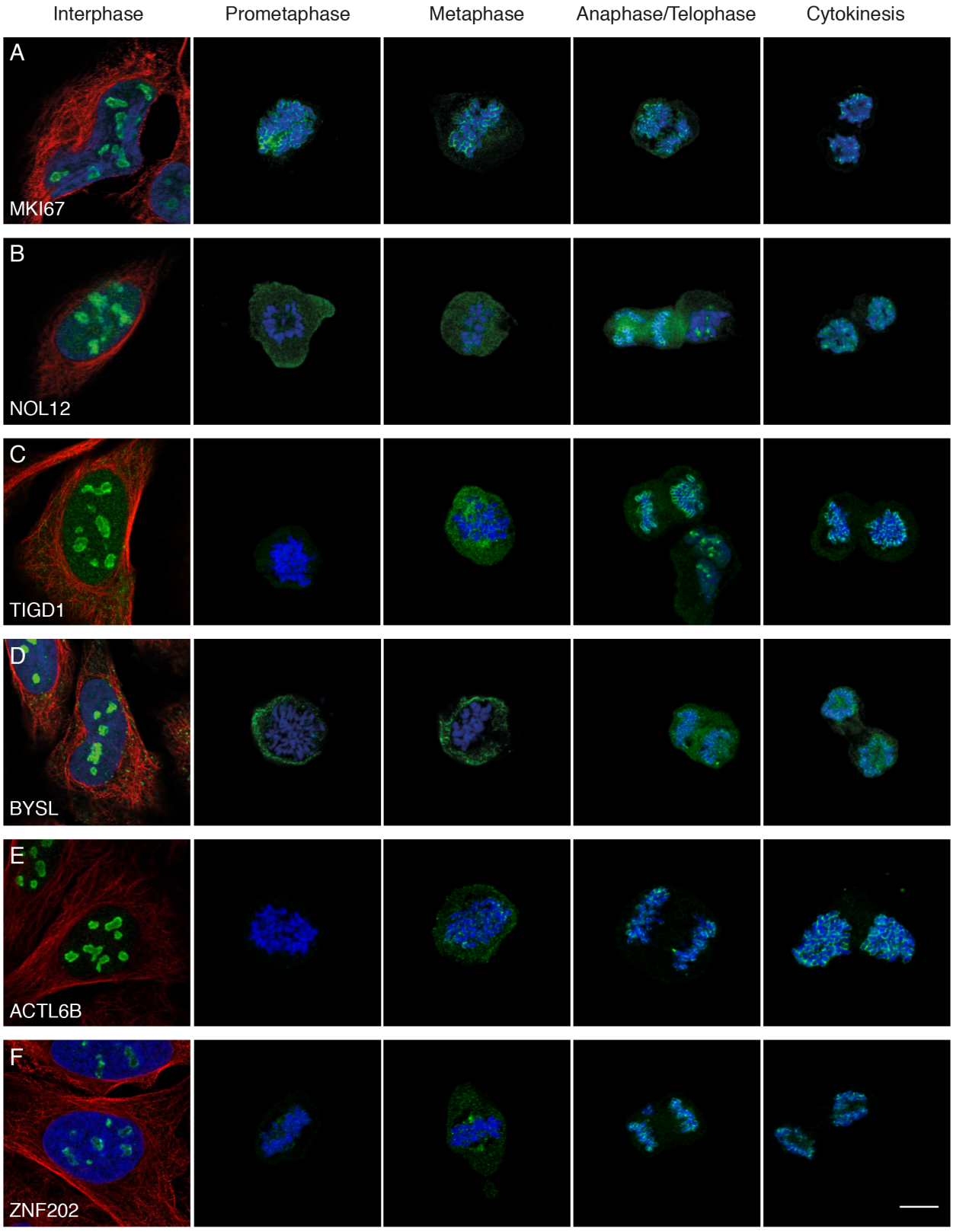

Figure 6 - Two expression phenotypes among mitotic chromosome proteins revealed. Protein of interest is shown in green, microtubules in red and DAPI in blue. Images of interphase cells were acquired from a different experiment and staining intensities cannot be compared between interphase and mitotic cells. Scale bar 10 µm. A) MKI67 is detected on the chromosomes throughout all mitotic phases and exemplifies proteins in the early onset category. B-F) The localization of B) NOL12, C) TIGD1, D) BYSL, E) ACTL6B, and F) ZNF202 to the chromosomes is only seen after metaphase, showing a typical late onset expression pattern.

All mitotic chromosome proteins need MKI67 as scaffold for binding

MKI67 is needed for proper chromosome segregation during mitosis. Previous studies have also shown that the perichromosomal layer cannot form in cells lacking MKI67 expression. As a consequence, this leads to disrupted localization of the other constituents of the perichromosomal layer (Booth *et al.*, 2014). As this study analyzed seven proteins only we wanted to investigate the behavior of all 65 mitotic chromosome proteins. This was done by using the same mitotic shake off protocol mentioned earlier but with a HeLa MKI67 knock-out (KO) cell line. All mitotic chromosome proteins were also stained in HeLa wild type (WT) cells to be used as a positive control. For all of the proteins being expressed on transcript level in HeLa WT cells (62 proteins) we could confirm the mitotic chromosome localization and for 53 proteins we could confirm the early and late recruitment. The timing of the recruitment for the remaining 9 proteins could not be confirmed due to too few mitotic cells not covering all mitotic phases. As expected for the KO cells, none of the 62 proteins could be fully recruited to the perichromosomal layer as the proteins form aggregates instead. Here exemplified by two already known constituents of the perichromosomal layer, PES1 and GNL3 (Fig. 7A-B) (Lerch-Gaggl *et al.*, 2002; Takata *et al.*, 2007). As opposed to the WT cells, the protein in the KO cells cannot be fully recruited to the chromosomal periphery while the nucleolus is mostly kept in its liquid-phase as aggregates throughout cell division. Interestingly, the temporal partitioning with early and late recruitment of proteins to the mitotic chromosomes can no-longer be observed in the MKI67 KO cells. For example DENN4A, EBNA1BP2 and NOL12 within the late recruitment category show a disrupted

mitotic chromosome location throughout all mitotic phases (identical to the early onset proteins PES1 and GNL3 (Fig. 7A-B)), not only from anaphase and onwards as in the HeLa WT cells (Fig. 7C-E, Fig. S13 for siRNA validation of EBNA1BP2 antibody). This result suggests that the expression of MKI67 could be important for these proteins to be redistributed to the perichromosomal layer during mitosis.

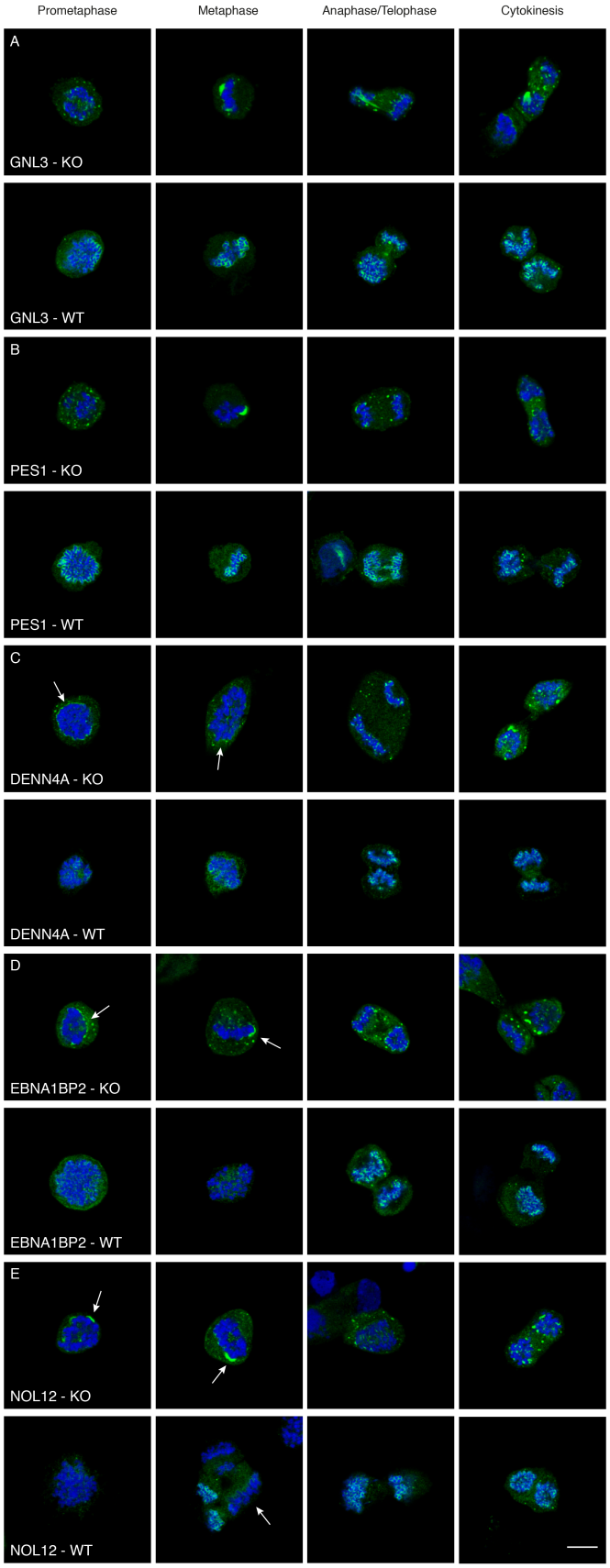

Figure 7 - Mitotic chromosome proteins in the MKI67 KO cell line. Protein of interest is shown in green and DAPI in blue. A) GNL3 and B) PES1 are localizing to protein aggregates around the chromosomes in the KO cells. C)-E) Late recruited proteins do not follow the same expression pattern in the KO cells compared to WT cells. Exemplified by C) DENN4A, D) EBNA1BP2 and E) NOL12.

Discussion

In this study we provide a single cell, image-based catalogue of the nucleolar proteome with a refined spatial resolution of the nucleolar substructures. This resource is made freely available as part of the Human Protein Atlas (www.proteinatlas.org). We provide evidence for 1203 nucleolar proteins currently not annotated as nucleolar in GO. We conclude that the nucleoli rim is not only a result of faulty antibody stainings as a similar pattern also can be seen in tagged cell lines. As the rim characteristic is enhanced in PFA fixed cells, which is known to affect solubility and charge of proteins, and that these proteins show a tendency to be more disordered than the other nucleolar proteins, these proteins might have common molecular features and function that remains to be unraveled. Another interesting finding is the overrepresentation of rim proteins being recruited to the perichromosomal layer during mitosis. A previous study shows that proteins residing in the granular component, in this case DDX21 and NCL, redistribute to the nucleoli rim upon knock-down of the nucleolar scaffold protein WDR46 (Hirai *et al.*, 2013). This further suggests that the localization to nucleoli rim also could be context dependent.

To understand the dynamics of nucleolar temporal reorganization, we mapped a subset of the nucleolar proteins during cell division. A considerable fraction of the protein targets (n = 65) were identified on the chromosomal periphery, of which 20 showed a late onset in terms of their chromosomal recruitment. This novel observation was enabled by the single cell imaging approach and has previously been overlooked by mass spectrometry-based studies of proteins on the perichromosomal layer.

Additionally, the late recruitment appears to be disrupted upon depletion of MKI67. Most likely due to the perichromosomal layer not being able to form properly in the absence of MKI67 (Booth *et al.*, 2014), which gives implications in the recruitment of these proteins. Little is still known about the function of the mitotic chromosomal surface and incorporating temporal resolution will allow further stratifications of the proteomic composition as it is likely that they are performing a variety of different functions. We speculate that some of the identified proteins are hitchhikers ensuring an even protein distribution in the daughter cells as the nucleolar protein aggregates in MKI67 deficient cells has shown to result in an uneven distribution of proteins after mitosis (Booth *et al.*, 2014). The proteins with a later recruitment could facilitate the assembly of the nucleolus during mitotic exit. Previous studies show that pre-nucleolar bodies are formed on the chromosomal periphery during telophase (Savino *et al.*, 2001; Angelier *et al.*, 2005; Sirri *et al.*, 2016). Proteins showing a late chromosomal recruitment might hence be needed for the early reformation of the nucleolus after cell division. One essential protein for nucleoli reformation is EBNA1BP2 (Chatterjee, Freeman and Busch, 1987), which in our data shows an increased recruitment on the mitotic chromosomes, peaking after metaphase. This suggests that proteins such as NOL12 with a similar expression pattern also are needed for nucleolar reassembly.

We show for the first time on a proteome-wide level that nucleolar proteins in general, and those migrating to mitotic chromosomes in particular, are more disordered compared to other proteins. Given that the nucleolus is dependent on liquid-liquid transitions to keep its spatial integrity, this result serves as an indication that the perichromosomal layer also acts as a liquid-like layer to separate the mitotic chromosomes during mitosis. Not surprisingly, MKI67 is highly disordered and given previous studies of the protein drivers for phase separation (Berry *et al.*, 2015; Elbaum-Garfinkle *et al.*, 2015; Lin *et al.*, 2015; Molliex *et al.*, 2015; Nott *et al.*, 2015), it is likely that other disordered proteins also play a key role in coating the chromosomes and facilitating liquid-liquid interactions. However, it should be noted that proteins predicted

to be highly disordered are not always active in phase separation as these are sensitive processes dependent on local environment and context. Therefore both *in vitro* and *in vivo* studies of individual proteins are needed to elucidate their phase separation promoting ability.

This freely available resource of the human nucleolar proteome can be used to gain better insights to the functions of the multi-facetted nucleolus. For instance, understanding the molecular dynamics of chromosome segregation and the role nucleolar proteins play on the perichromosomal layer during mitosis.

Acknowledgment

We acknowledge the entire staff of the Human Protein Atlas program. We also thank staff at the Chan-Zuckerberg Biohub and the Allen Institute for Cell Science for fruitful discussions on the nucleolus. Funding was provided by the Knut and Alice Wallenberg Foundation (2016.0204) and Swedish Research Council (2017-05327) to E.L.

Author contributions

E.L conceived the study. E.L and L.S. developed methodology and carried out data investigation. L.S. conducted experimental work and data analysis. D.M. advised and conducted experimental work for the mitotic shake off protocol and data analysis. C.G. and M.L. generated and imaged tagged cell lines for nucleoli rim investigation. S.C.H. developed and provided the MKI67 KO cell line and advised experimental work and data analysis. L.S. created the figures. E.L. and L.S did manuscript writing. C.G., D.M., M.U., P.T and S.C.H. revised the manuscript. E.L. supervised and administered project and funding.

Conflict of interest

The authors declare no conflicts of interest.

Material and Method

HPA Cell Atlas workflow

Antibody generation

Most antibodies used for the immunofluorescent experiments were affinity purified using the antigen as ligand, rabbit polyclonal antibodies produced and validated within the Human Protein Atlas project (Uhlen *et al.*, 2010). The commercial antibodies used were handled according to the supplier's recommendations.

Cell line cultivation

The cells were grown at 37 °C in a 5 % CO_2 environment. The cultivation media used for each cell line was recommended by the supplier with an addition of 10 % Fetal Bovine Serum (FBS, VWR, Radnor, PA, USA). For immunostaining, cells were seeded onto 96-well glass bottom plates (Whatman, GE Healthcare, UK, and Greiner Sensoplate Plus, Greiner Bio-One, Germany) coated with 12.5 µg/ml fibronectin (VWR) and incubated between 4-20 h dependent on cell line before fixation.

Image acquisition and annotation

Image acquisition was performed using a Leica SP5 DM6000CS confocal microscope equipped with a 63x HCX PL APO 1.4 CS oil immersion objective. At least two representative images from each well were acquired using the following settings; Pinhole 1 Airy unit, 16 bit, 600 Hz, line average 2 and a pixel size of 80 nm. The gain (maximum 800 V) was kept the same for all images for one antibody. The images for each protein were then manually evaluated based on staining intensity, subcellular location and expression pattern. In total, the HPA Cell Atlas database consists of immunofluorescent stainings of more than 12 000 proteins mapped to 33 different subcellular structures. In this study, only proteins localizing to any nucleolar structure have been analyzed. Due to the image resolution, the fibrillar center annotation is used as a collective term for proteins located to either the FC or DFC of the nucleoli. Nucleoli rim and mitotic chromosome is not a public annotation in the HPA v19 but the data presented in this paper can be found in Table S1 and Table S3 respectively.

Classification of protein location reliability

All antibodies passing initial quality controls such as reproducibility between cell lines, correlation between signal intensity and RNA expression, reproducibility between antibodies binding different epitopes of the proteins or agreement with validation data such as siRNA knockdown, was given a reliability score. All detected localizations were given any of the following scores; enhanced, supported, approved or uncertain. Locations within the "enhanced" category have been experimentally confirmed by at least one of the methods within the validation pillars for antibodies (Uhlen *et al.*, 2016), the most common being genetic knockdown or an independent antibody. A "supportive" score was given if the location in question can be confirmed by external experimental data from the Swissprot database (The UniProt Consortium, 2019). If no external data is available, the location scored as "approved" and if the location is contradictory to existing literature or that the RNA expression of the protein is low, the location got the "uncertain" label.

Mitotic chromosome localization

To investigate nucleolar protein localization during mitosis, U-2 OS cells were cultivated in the same conditions as described above using Modified Mc Coy's 5A Medium (M8403, Sigma Aldrich) + 10 % FBS + 1 % L-glutamine (G7513, Sigma Aldrich). Before seeding onto the 96-well glass plate, the cells were gently shaken in the cultivation plate to detach the mitotic cells. After centrifugation at 1700 rpm for three minutes, the mitotic cells were seeded and directly fixed with 4% PFA for 15 minutes at room temperature. After fixation, the IF staining protocol was carried out as described above. The 150 protein targets were chosen either by having a documented connection to MKI67 or the MKI67 interacting protein NIFK in a protein-protein association network or showing a nucleoli rim staining similar to MKI67 in interphase. The secondary antibody used was Alexa anti-rabbit 488 and cells were also counterstained with DAPI. Images of mitotic cells in prometaphase, metaphase, anaphase/telophase and cytokinesis were acquired with 63x magnification with the same imaging settings as previously described. Since cells were fixed, the classification of the different cell cycle phases is an estimation based on the nuclear morphology. The same gain was used to image all mitotic cells for

each protein. Due to enrichment of only mitotic cells in the experiment, images of interphase cells for the same protein are taken from another experiment. Hence the images are acquired with a different gain and staining intensities are not comparable.

MKI67 tagged cell line generation

Cell Cultivation of Hek293T$^{mNG1-10}$ cells

Hek293T cells stably expressing mNG1-10 were cultured in high-glucose Dulbecco's Modified Eagle Medium supplemented with 10 % FBS, 1 mM glutamine and 100 µg/ml penicillin/streptomycin (Gibco). Cells were maintained in 96-well plates at 37 °C in a 5.0 % CO_2 humidified environment.

Nucleic acid reagents and gene constructs

All synthetic nucleic acid reagents (Table S4) were ordered from Integrative DNA Technologies (IDT DNA). Cells were endogenously tagged at the N- or C-terminus for MKi67 and GNL3 respectively. The 90 bp insert consisted of a C- or N- terminal linker, the mNG11 sequence and a protease linker.

RNP preparation and electroporation

Cas9/sgRNA ribonucleo-protein complexes were prepared according to established methods by assembling 100 pmol Cas9 protein and 130 pmol sgRNA (Leonetti *et al.*, 2016). SgRNA was diluted in 6.5 ul Cas9 buffer (150 mM KCl, 20 mM Tris pH 7.5, 1 mM TCEP-Cl, 1 mM $MgCL_2$, 10% glycerol) and incubated at 70 °C for 5 min. After addition of the Cas9 protein, the RNP assembly was performed at 37 °C for 10 min. 1 µl of HDR template was added to a total volume of 10 µl. Hek293T$^{mNG1-10}$ cells were treated with 200 ng/mL nocadozole (Sigma) for 16 hours prior electroporation. Electroporation was carried out according to manufacturer's instructions using SF-cell line reagents (Lonza) in an Amaxa 96-well shuttle Nucleofector device (Lonza). Cells were washed with PBS and resuspended to 10^4 cells/µl in SF solution. $2x10^5$ cells were mixed with the Cas9/sgRNA RNP complexes, electroporated using the CM-130 program and rescued in cell culture medium in a 96 well plate. Electroporated cells were cultured and maintained for 8 days prior to FACS analysis.

Fluorescence activated cell sorting (FACS) and clonal enrichment

We performed analytical flow cytometry on a Sony SH800 instrument to assess the tagging efficiency of the cell lines. Singlets and live cells were analysed. Clonal populations of the 0.5% highest mNG-expressing cells were established by sorting single cells in the wells of a 96-well plate.

Generation of Illumina amplicon sequencing libraries

DNA repair outcomes were characterized by Illumina amplicon Sequencing. Cells were grown in a 96-well plate at around 80% confluency. Medium was aspirated and cells were washed with PBS. Cells were thoroughly resuspended in 50 µl QuickExtract (Lucigen) and incubated at 65 °C for 20 min and 98 °C for 5 min. 2 µl gDNA, 20 µl 2x KAPA, 1.6 µl of 50 µM forward and reverse primer, 8 µl 5 M betaine and 8.4 µ H_2O were run using the following thermocycler settings: 3 min at 95 °C followed by 3 cycles of 20 s at 98 °C, 15 s at 63 °C 20 s at 72 °C, 3 cycles of 20 s at 98 °C, 15 s at 65 °C 20 s at 72 °C, 3 cycles of 20 s at 98 °C, 15 s at 67 °C 20 s at 72 °C and 17 cycles of 20 s at 98 °C, 15 s at 69 °C 20 s at 72 °C. A barcoding PCR was carried out to append unique index sequences to each amplicon for multiplexed sequencing. 1 µl of 2 nM PCR product, 4 µl of forward and reverse indexed barcoding primer, 20 µl 2x Kapa and 11 µl H_2O were run with the following thermocycler settings: 3 min at 95 °C, 10 cycles of 20 s at 98 °C, 15 s at 68 °C, 12 s at 72 °C. Product concentrations in 200 – 600 bp range were quantified using a Fragment Analyzer (Agilent) and pooled at 500 nM. Amplicon sequencing library was purified using Solid Phase Reversible Immobilization at a 1.1x bead/sample ratio. Sequencing was performed using an Illumina MiSeq system at the CZ Biohub Sequencing facility. Sequencing outcomes were characterized using CRISPResso (Pinello *et al.*, 2016). Only homozygous HDR repaired cell lines, or heterozygous repaired cell lines with the other allele(s) being unmodified were selected for follow up experiments.

Spinning-disk confocal live cell microscopy

20000 endogenously tagged HEK293T cells were grown on a fibronectin (Roche)-coated 96-well glass bottom plate (Cellvis) for 24 hours. Cells were counter-stained in 0.5 µg/ml Hoechst 33342 (Thermo) for 30 min at 37 °C and imaged in complete DMEM

without phenol-red. Live-cell imaging was performed at 37 °C and 5% CO_2 on a Dragonfly spinning-disk confocal microscope (Andor) equipped with a 1.45 N/A 63x oil objective and an iXon Ultra 888 EMCCD camera (Andor).

To compare the presence of the nucleolar rim of mNG tagged proteins in live and fixed cells we fixed mNG tagged cells in 4% formaldehyde (Thermo Scientific, 28908).

MKI67 KO cell line generation

MKI67 HeLa KO cells were developed and kindly donated by Dr. Cuylen. Details about generation and validation of the cells is described in (Cuylen *et al.*, 2016).

Data analysis

Gene Ontology and functional enrichment

The web-based tool QuickGO (Binns *et al.*, 2009) was used to check the overlap with our nucleolar genes and nucleolar genes labeled as experimentally verified on GO (GO:0005730, Data downloaded November 22nd 2019). The GO annotations based on data from the Cell Atlas were removed before comparison. The functional annotation clustering for the nucleolar genes was performed using the web-based tool DAVID (Database for Annotation, Visualization, and Integrated Discovery v. 6.8) (D. Huang, Sherman and Lempicki, 2009; D. W. Huang, Sherman and Lempicki, 2009). All human genes were used as a background. The GO domain “biological process” terms with a Bonferroni value of less than 0.01 was regarded as significantly enriched.

Intrinsic disorder prediction

Protein disorder was predicted using IUPRED2A (Bálint, Gábor and Dosztányi, 2018). The disorder level was predicted to the nucleolar, nucleoli rim, fibrillar center and mitotic chromosome proteins and compared to 2054 non-nuclear cytosolic proteins as defined in the HPA Cell Atlas (v19). The mitotic chromosome proteins were removed from the nucleolar dataset prior data analysis to avoid redundancy. The output from IUPRED2A gives a probability score between 0-1 for each protein residue, where a score above 0.5

indicates disorder. The number of disordered residues per protein was divided by the protein length to get the disorder fraction. A Kruskal Wallis test followed by Dunn's test with Bonferroni correction was used to compute statistical significance.

Functional protein association network

The functional protein association networks were created using the STRING app v 1.4.2 in Cytoscape v 3.7.1. (Doncheva *et al.*, 2019).

Pan dependency analysis

The estimation of pan-dependent genes within the mitotic chromosome protein dataset was performed using the essential gene information from the DepMap Achilles 19Q1 Public dataset (Meyers *et al.*, 2017). A pan-dependent gene is defined as "those for whom 90% of cell lines rank the gene above a given dependency cutoff. The cutoff is determined from the central minimum in a histogram of gene ranks in their 90th percentile least dependent line". The fraction of essential genes in the mitotic chromosome dataset and the nucleolar genes was computed and a Pearson's Chi Squared test was performed to state the statistical significance.

Prognostic cancer marker analysis

The prognostic cancer marker analysis was based on data from the HPA Pathology Atlas (Uhlen *et al.*, 2017)**.** To estimate each gene's prognostic potential, patients were classified into two expression groups based on the FPKM value of each gene and the correlation between expression level and patient survival was examined. Genes with a median expression less than FPKM 1 were excluded. The prognosis of each group of patients was examined by Kaplan-Meier survival estimators, and the survival outcomes of the two groups were compared by log-rank tests. Genes with log rank p-values less than 0.001 in maximally separated Kaplan-Meier analysis were defined as prognostic genes. If the group of patients with high expression of a selected prognostic gene has a higher observed event than expected event, it is an unfavorable prognostic gene; otherwise, it is a favorable prognostic gene. The full list of favorable and unfavorable prognostic genes were downloaded from the HPA website (v.19, proteinatlas.org). The

fraction of unfavorable genes within the mitotic chromosome dataset was compared to the fraction for all nucleolar genes and all human genes respectively. A Pearson's Chi Squared test was carried out to compute the statistical significance.

Figure generation

Plots were generated using R (v. 3.6.1), R studio (v. 1.0.136) and the additional ggplot2 package. The image montages were created using FIJI ImageJ (v. 2.0.0-rc-69/1.52n).

Supplemental Information

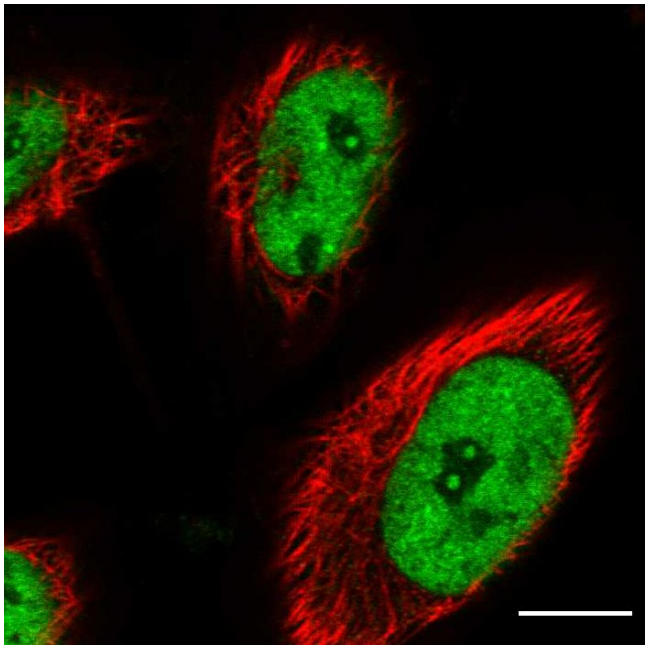

Supplementary Figure 1

Immunofluorescent staining of LEO1 in HeLa wild type cells. Protein of interest is shown in green and microtubules in red. Scale bar 10 μm.

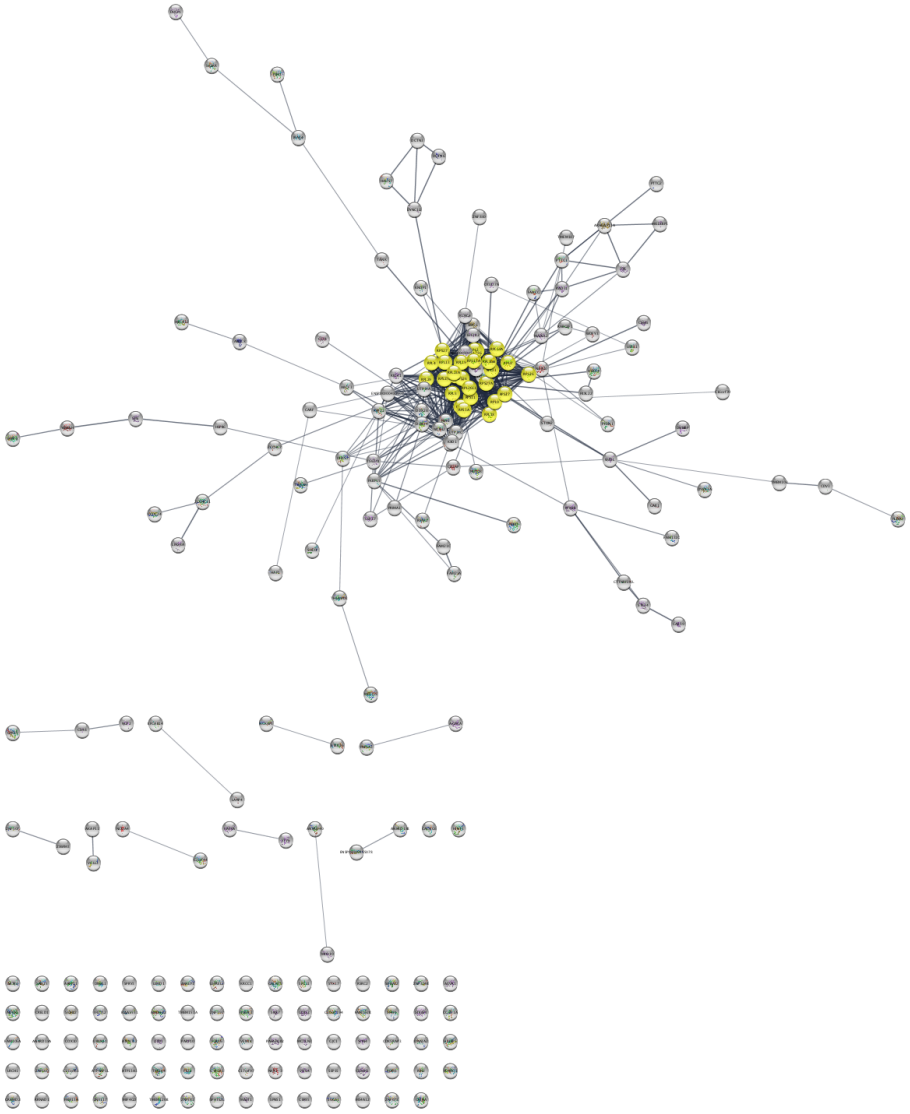

Supplementary Figure 2

Protein-protein association network of the shared nucleolar and cytosolic proteome. The yellow highlighted nodes show ribosomal proteins.

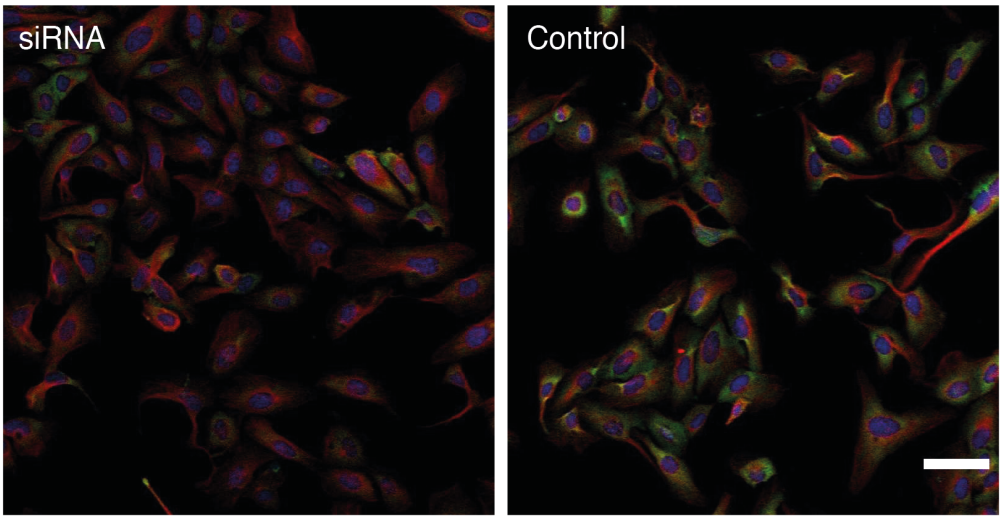

Supplementary Figure 3

siRNA antibody validation data for RPL13. siRNA treated cells to the left, control cells to the right. Protein of interest is shown in green, microtubules in red and DAPI in blue. Scale bar 20 µm.

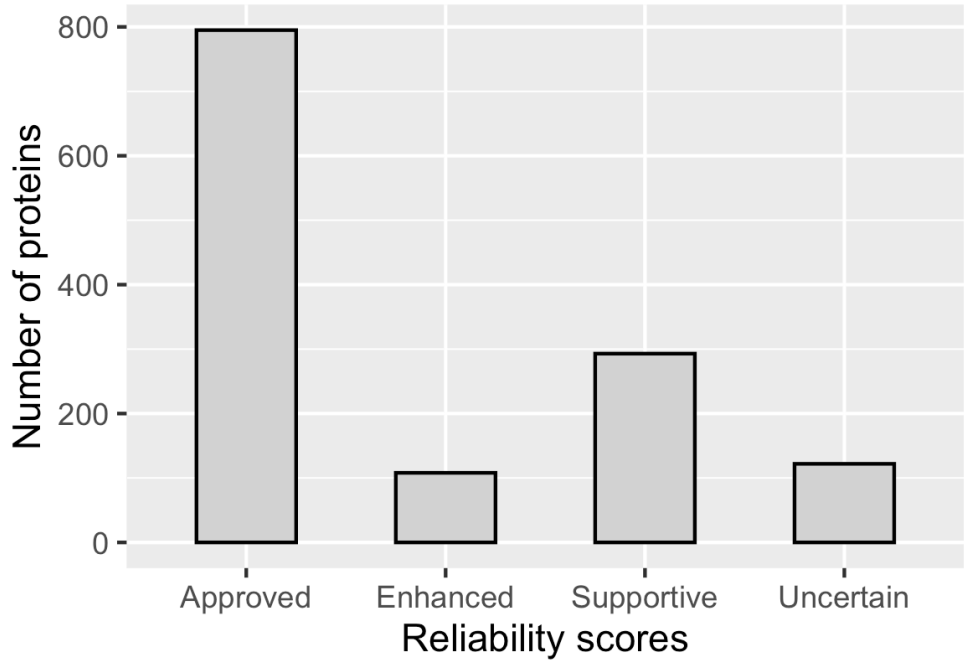

Supplementary Figure 4

Distribution of the localization reliability scores for the nucleolar proteins in the HPA Cell Atlas (v.19).

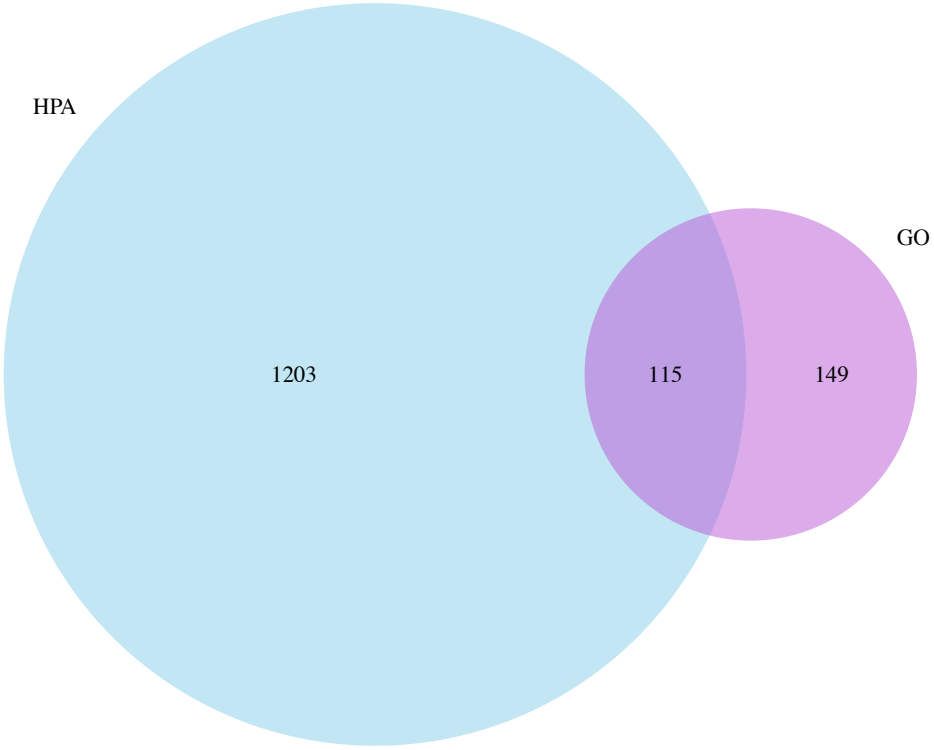

Supplementary Figure 5

Overlap between genes with an experimentally verified nucleolar localization in Gene Ontology and the nucleolar dataset in the HPA Cell Atlas.

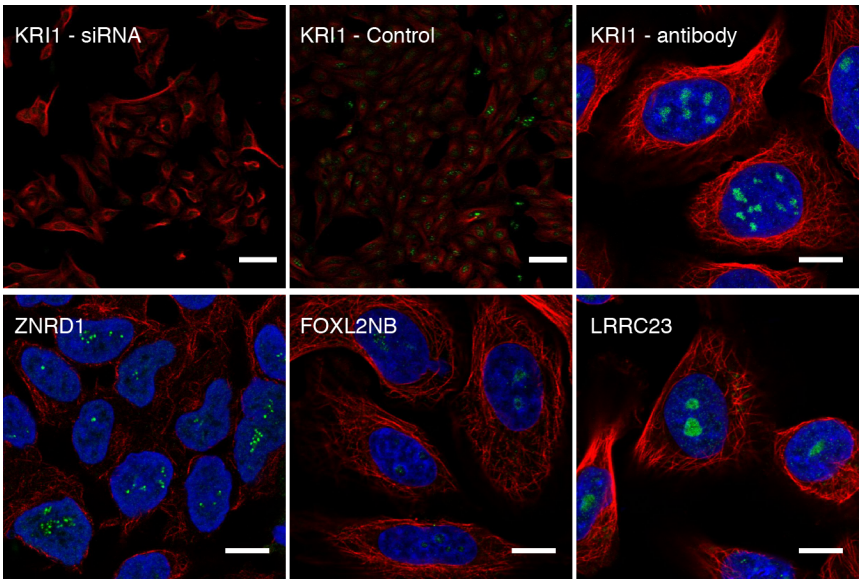

Supplementary Figure 6

siRNA antibody validation data for KRI1. siRNA treated cells to the left, control cells to the right. Scale bar 20 µm.

Additional IF stainings of KRI1, ZNRD1, FOXL2NB and LRRC23 using antibodies targeting different epitopes of the protein showing the same localization pattern as the original antibody. Protein of interest is shown in green, microtubules in red and DAPI in blue. Scale bar 10 µm.

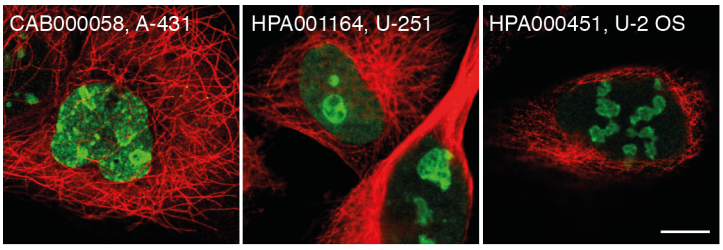

Supplementary Figure 7

IF stainings of MKI67 using three antibodies targeting different epitopes of the protein. All showing the characteristic nucleoli rim staining pattern. Protein of interest is shown in green and microtubules in red. Scale bar 10 µm.

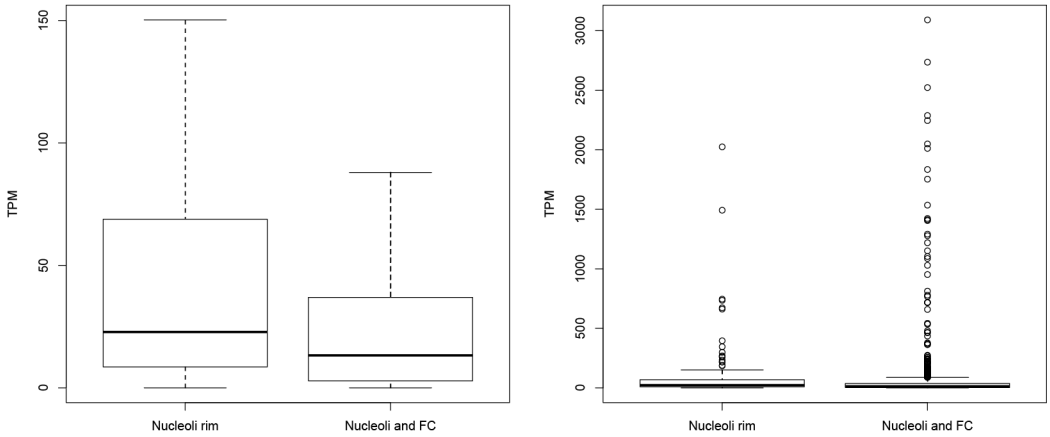

Supplementary Figure 8

RNA expression data (in TPM) for the nucleoli rim proteins compared to the other nucleolar proteins. The left box plot shows the distribution of quartile one to four, while the right box plot shows the distribution of all genes in the dataset.

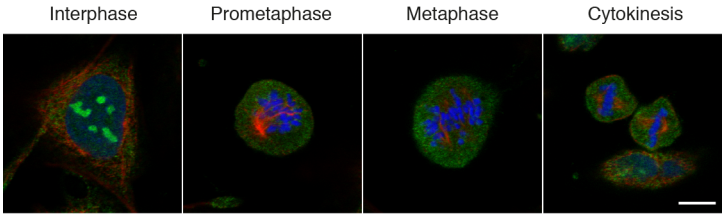

Supplementary Figure 9

85 out of 150 nucleolar proteins did not localize to mitotic chromosomes. Here exemplified by RPS19BP1. Protein is shown in green, DAPI and blue and microtubules in red. Scale bar 10 µm.

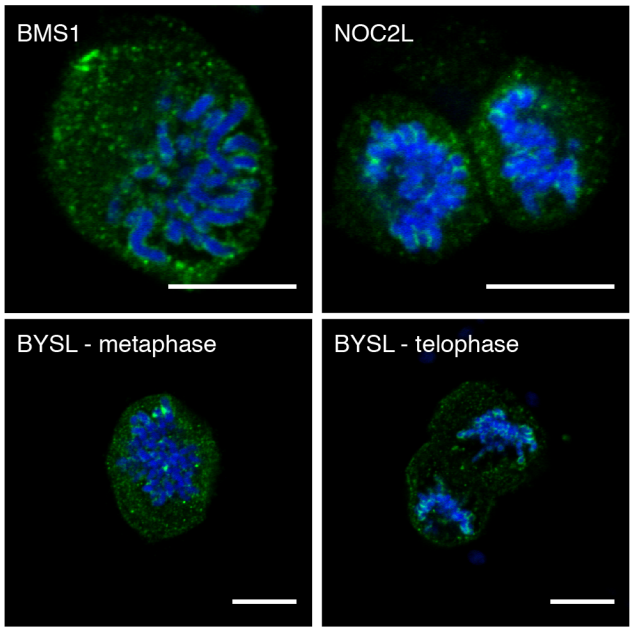

Supplementary Figure 10

Additional IF stainings of BMS1, NOC2L and BYSL in mitosis using antibodies targeting different epitopes of the protein showing the same localization on mitotic chromosomes as the original antibody. Protein of interest is shown in green and DAPI in blue. Scale bar 10 µm.

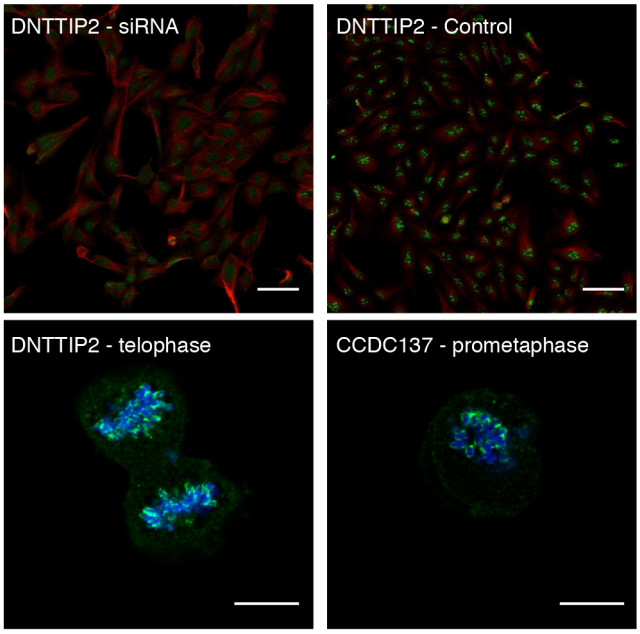

Supplementary Figure 11

siRNA antibody validation data for DNTTIP2. siRNA treated cells to the left, control cells to the right. Scale bar 20 µm.

IF stainings of DNTTIP2 and CCDC137 in mitotic cells showing localization to mitotic chromosomes. Protein of interest is shown in green and DAPI in blue. Scale bar 10 µm.

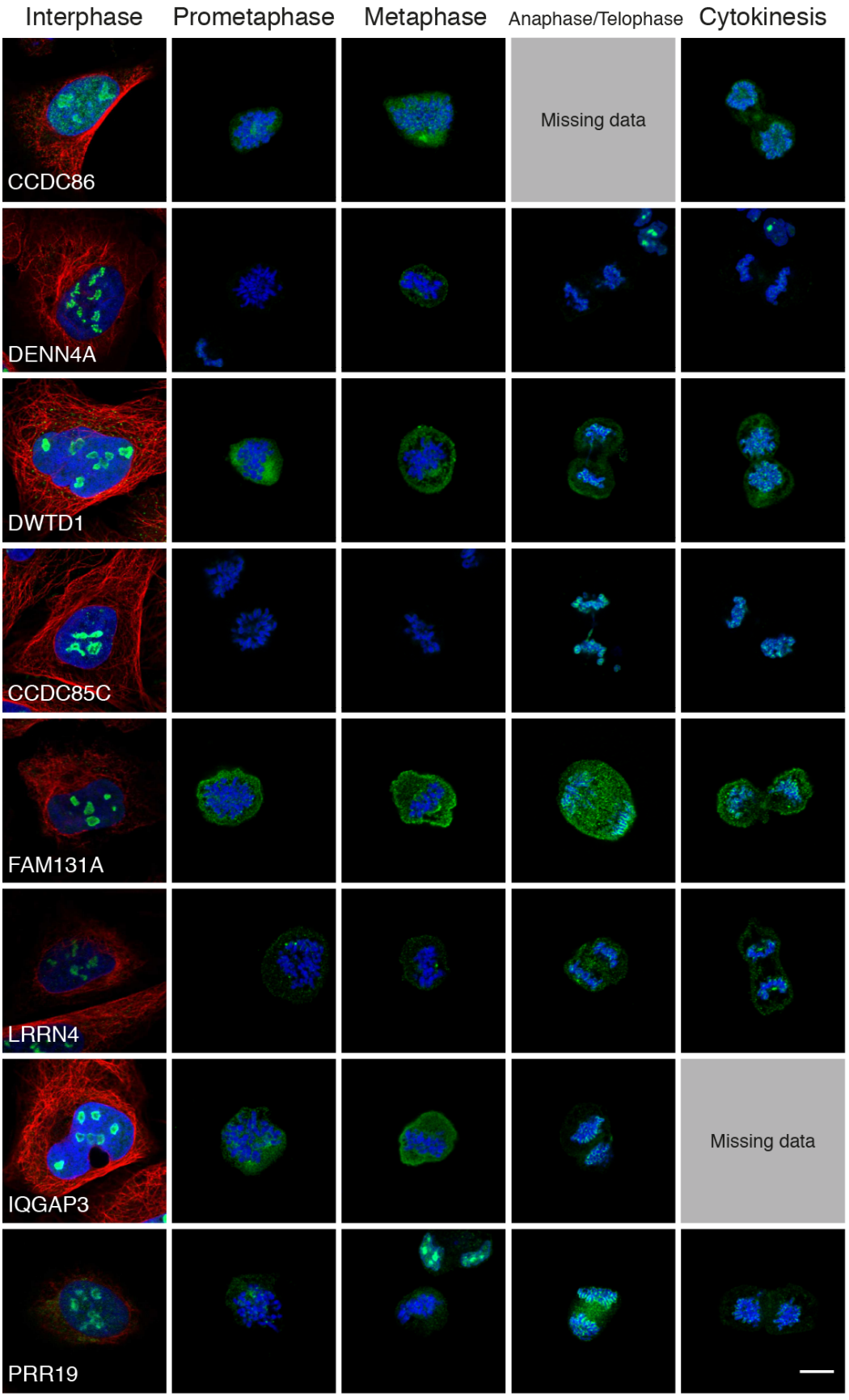

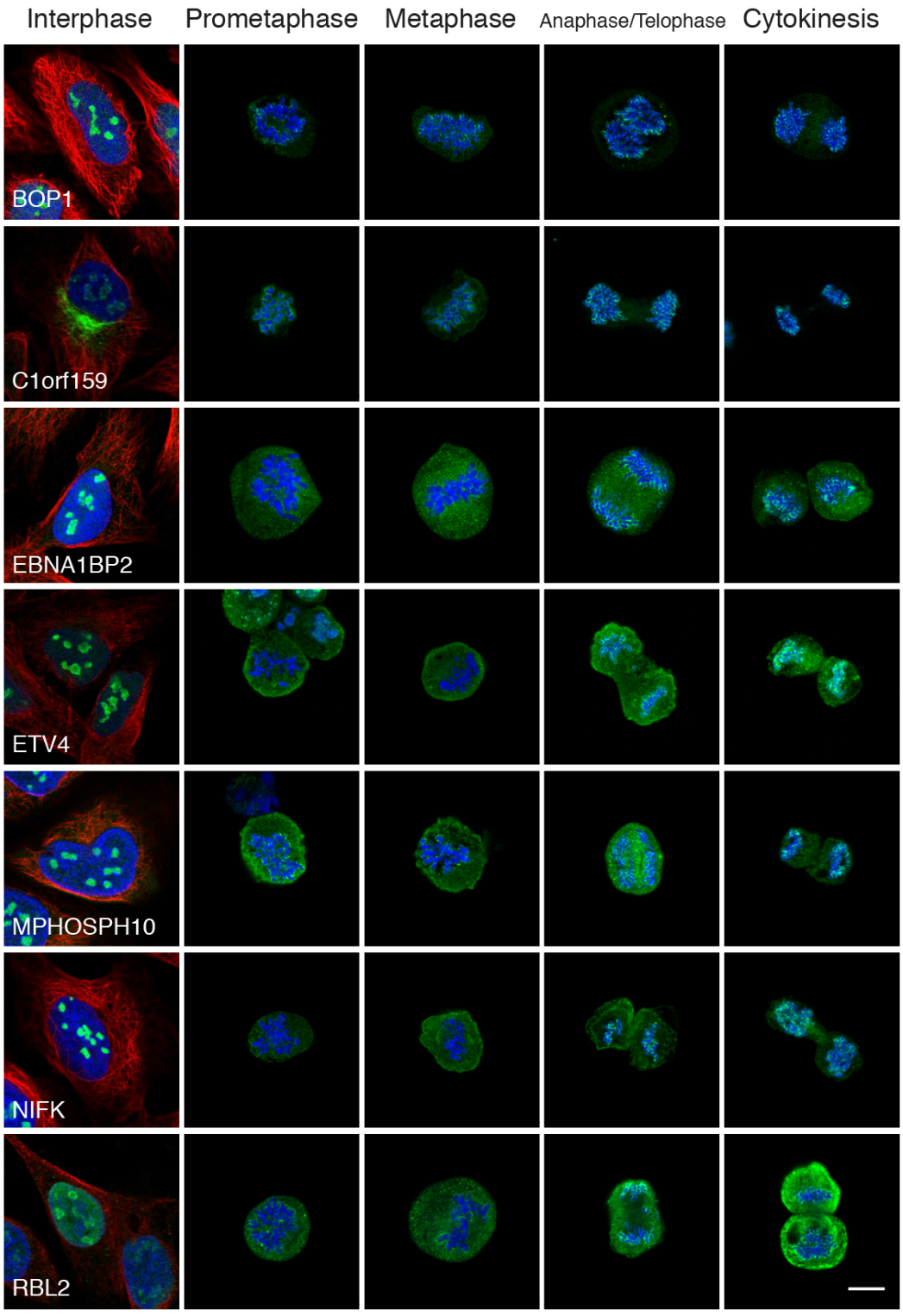

Supplementary Figure 12

IF stainings of the proteins showing a late recruitment to mitotic chromosomes. Protein of interest is shown in green, microtubules in red and DAPI in blue. Images of interphase cells

were acquired from a different experiment and staining intensities cannot be compared between interphase and mitotic cells. Scale bar 10 µm.

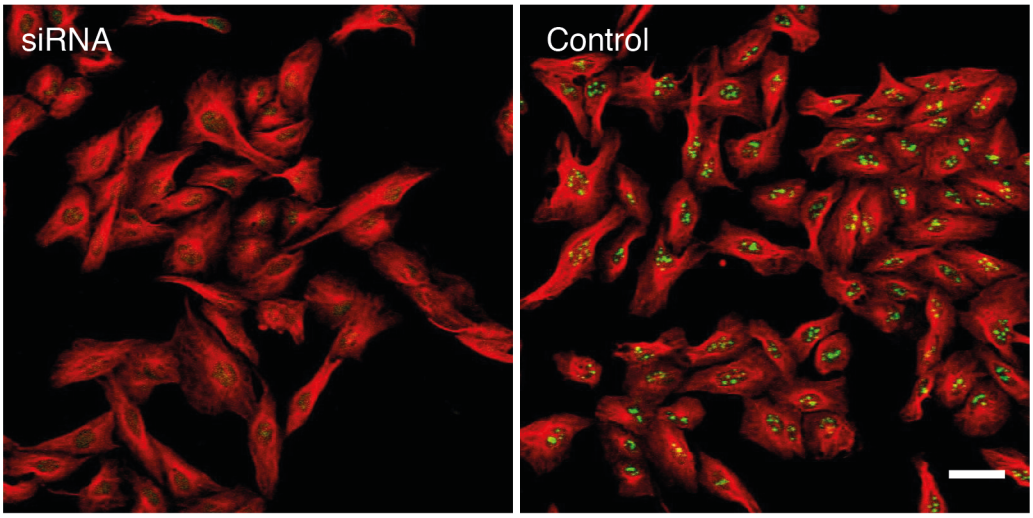

Supplementary Figure 13

siRNA antibody validation data for EBNA1BP2. siRNA treated cells to the left, control cells to the right. Protein of interest is shown in green and microtubules in red. Scale bar 20 µm.

References

Amin, M. A., Matsunaga, S., Uchiyama, S. and Fukui, K. (2008) 'Depletion of nucleophosmin leads to distortion of nucleolar and nuclear structures in HeLa cells', *Biochemical Journal*, 415(3), pp. 345–351.

Andersen, J. S., Lam, Y. W., Leung, A. K. L., Ong, S.-E., Lyon, C. E., Lamond, A. I. and Mann, M. (2005) 'Nucleolar proteome dynamics', *Nature*, 433(7021), p. 77.

Andersen, J. S., Lyon, C. E., Fox, A. H., Leung, A. K. L., Lam, Y. W., Steen, H., Mann, M. and Lamond, A. I. (2002) 'Directed proteomic analysis of the human nucleolus', *Current Biology*, 12(1), pp. 1–11.

Angelier, N., Tramier, M., Louvet, E., Coppey-Moisan, M., Savino, T. M., De Mey, J. R. and Hernandez Verdun, D. (2005) 'Tracking the interaction of rRNA processing proteins during nucleolar assembly in living cells', *Molecular Biology of the Cell*, 16(6), pp. 2862–2871.

Bálint, M., Gábor, E. and Dosztányi, Z. (2018) 'IUPred2A: context-dependent prediction of protein disorder as a function of redox state and protein binding', *Nucleic Acids Research*, 46(W1), pp. W329–W337.

Berry, J., Weber, S. C., Vaidya, N., Haataja, M. and Brangwynne, C. P. (2015) 'RNA transcription modulates phase transition-driven nuclear body assembly', *Proceedings of the National Academy of Sciences*, 112(38), pp. E5237–E5245.

Binns, D., Dimmer, E., Huntley, R., Barrell, D., O'Donovan, C. and Apweiler, R. (2009) 'QuickGO : a web-based tool for Gene Ontology searching', *Bioinformatics*, 25(22), pp. 3045–3046.

Boisvert, F. M., Van Koningsbruggen, S., Navascués, J. and Lamond, A. I. (2007) 'The multifunctional nucleolus', *Nature Reviews Molecular Cell Biology*, 8(7), pp. 574–585.

Booth, D. G., Beckett, A. J., Molina, O., Samejima, I., Masumoto, H., Kouprina, N., Larionov, V., Prior, I. A. and Earnshaw, W. C. (2016) '3D-CLEM reveals that a major portion of mitotic chromosomes is not chromatin', *Molecular Cell*. Elsevier Inc., 64(4), pp. 790–802.

Booth, D. G., Takagi, M., Sanchez-Pulido, L., Petfalski, E., Vargiu, G., Samejima, K., Imamoto, N., Ponting, C. P., Tollervey, D., Earnshaw, W. C. and Vagnarelli, P. (2014) 'Ki-67 is a PP1-interacting protein that organises the mitotic chromosome periphery', *eLife*, 3, p. e01641.

Brangwynne, C. P., Eckman, C. R., Courson, D. S., Rybarska, A., Hoege, C., Gharakhani, J., Jülicher, F. and Hyman, A. A. (2009) 'Germline P granules are liquid droplets That localize by controlled dissolution/condensation', *Science*, 324(5935), pp. 1729–1732.

Brangwynne, C. P., Mitchison, T. J. and Hyman, A. A. (2011) 'Active liquid-like behavior of nucleoli determines their size and shape in Xenopus laevis oocytes', *Proceedings of the National Academy of Sciences*, 108(11), pp. 4334–4339.

Caragine, C. M., Haley, S. C. and Zidovska, A. (2019) 'Nucleolar dynamics and interactions with

nucleoplasm in living cells', *eLife*, 8.

Chatterjee, A., Freeman, J. W. and Busch, H. (1987) 'Identification and partial characterization of a Mr 40, 000 nucleolar antigen associated with cell proliferation', *Cancer Research*, 47(4), pp. 1123–1129.

Cuylen, S., Blaukopf, C., Politi, A. Z., Müller-Reichert, T., Neumann, B., Poser, I., Ellenberg, J., Hyman, A. A. and Gerlich, D. W. (2016) 'Ki-67 acts as a biological surfactant to disperse mitotic chromosomes', *Nature*. Nature Publishing Group, 535(7611), p. 308.

Doncheva, N. T., Morris, J. H., Gorodkin, J. and Jensen, L. J. (2019) 'Cytoscape stringApp: Network analysis and visualization of proteomics data', *Journal of proteome research*. American Chemical Society, 18(2), pp. 623–632.

Dong, Z., Zhu, C., Zhan, Q. and Jiang, W. (2017) 'The roles of RRP15 in nucleolar formation , ribosome biogenesis and checkpoint control in human cells', 8(8), p. 13240.

Dragon, F., Gallagher, J. E. G., Compagnone-Post, P. A., Mitchell, B. M., Porwancher, K. A., Wehner, K. A., Wormsley, S., Settlage, R. E., Shabanowitz, J., Osheim, Y., Beyer, A. L., Hunt, D. F. and Baserga, S. J. (2002) 'A large nucleolar U3 ribonucleoprotein required for 18S ribosomal RNA biogenesis', *Science*, 417(6892), p. 967.

Elbaum-Garfinkle, S., Kim, Y., Szczepaniak, K., Chen, C. C.-H., Eckmann, C. R., Myong, S. and Brangwynne, C. P. (2015) 'The disordered P granule protein LAF-1 drives phase separation into droplets with tunable viscosity and dynamics', *Proceedings of the National Academy of Sciences*, 112(23), pp. 7189–7194.

Feric, M., Vaidya, N., Harmon, T. S., Mitrea, D. M., Zhu, L., Richardson, T. M., Kriwacki, R. W., Pappu, R. V. and Brangwynne, C. P. (2016) 'Coexisting liquid phases underlie nucleolar subcompartments', *Cell*. Elsevier Inc., 165(7), pp. 1686–1697.

Gambe, A. E., Matsunaga, S., Takata, H., Ono-maniwa, R., Baba, A., Uchiyama, S. and Fukui, K. (2009) 'A nucleolar protein RRS1 contributes to chromosome congression', *FEBS Letters*. Federation of European Biochemical Societies, 583(12), pp. 1951–1956.

Gautier, T., Dauphin-Villemant, C., André, C., Masson, C., Arnoult, J. and Hernandez-Verdun, D. (1992) 'Identification and characterization of a new set of nucleolar ribonucleoproteins which line the chromosomes during mitosis', *Experimental Cell Research*, 200(1), pp. 5–15.

Gautier, T., Masson, C., Quintana, C., Arnoult, J. and Hernandez-Verdun, D. (1992) 'The ultrastructure of the chromosome periphery in human cell lines', *Chromosoma*, 101(8), pp. 502–510.

Gautier, T., Robert-Nicoud, M., Guilly, M.-N. and Hernandez-Verdun, D. (1992) 'Relocation of nucleolar proteins around chromosomes at mitosis. A study by confocal laser scanning microscopy', *J Cell Sci*, 102(4), pp. 729–737.

Gerdes, J., Lemke, H., Baisch, H., Wacker, H. H., Schwab, U. and Stein, H. (1984) 'Cell cycle analysis of a cell proliferation-associated human nuclear antigen defined by the monoclonal antibody Ki-67', *The Journal of Immunology*, 133(4), pp. 1710–1715.

Hirai, Y., Louvet, E., Oda, T., Kumeta, M., Watanabe, Y., Horigome, T. and Takeyasu, K. (2013) 'Nucleolar scaffold protein, WDR46, determines the granular compartmental localization of nucleolin and DDX 21', *Genes to Cells*, 18(9), pp. 780–797.

Hirano, Y., Ishii, K., Kumeta, M., Furukawa, K., Takeyasu, K. and Horigome, T. (2009) 'Proteomic and targeted analytical identification of BXDC1 and EBNA1BP2 as dynamic scaffold proteins in the nucleolus', *Genes to Cells*, 14(2), pp. 155–166.

Van Hooser, A. A., Yuh, P. and Heald, R. (2005) 'The perichromosomal layer', *Chromosoma*, 114(6), pp. 377–388. doi: 10.1007/s00412-005-0021-9.
Huang, D., Sherman, B. and Lempicki, R. (2009) 'Bioinformatics Enrichment Tools: Paths Towards the Comprehensive Functional Analysis of Large Gene Lists', *Nucleic Acid Res.*, 37(1), pp. 1–13.

Huang, D. W., Sherman, B. T. and Lempicki, R. A. (2009) 'Systematic and integrative analysis of large gene lists using DAVID bioinformatics resources', *Nature protocols*, 4(1), p. 44.

Huh, W., Falvo, J. V., Gerke, L. C., Carroll, A. S., Howson, R. W., Weissman, J. S. and Shea, E. K. O. (2003) 'Global analysis of protein localization in budding yeast', *Nature*, 425(6959), p. 686.

Koiwai, K., Noma, S., Takahashi, Y., Hayano, T., Maezawa, S., Kouda, K., Matsumoto, T., Suzuki, M., Furuichi, M. and Koiwai, O. (2011) 'TdIF2 is a nucleolar protein that promotes rRNA gene promoter activity', *Genes to Cells*, 16(7), pp. 748–764.

Kwon, H. and Green, M. R. (1994) 'The RNA polymerase I transcription factor, upstream binding factor, interacts directly with the TATA Box-binding protein', *Journal of Biological Chemistry*, 269(48), pp. 30140–30146.

Leonetti, M. D., Sekine, S., Kamiyama, D., Weissman, J. S. and Huang, B. (2016) 'A scalable strategy for high-throughput GFP tagging of endogenous human proteins', *Proceedings of the National Academy of Sciences*, 113(25), pp. E3501–E3508.

Lerch-Gaggl, A., Haque, J., Li, J., Ning, G., Traktman, P. and Duncan, S. A. (2002) 'Pescadillo is essential for nucleolar assembly, ribosome Biogenesis, and mammalian cell proliferation', *Journal of Biological Chemistry*, 277(47), pp. 45347–45355.

Leung, A. K. L., Trinkle-Mulcahy, L., Lam, Y. W., Andersen, J. S., Mann, M. and Lamond, A. I. (2006) 'NOPdb: nucleolar proteome database', *Nucleic Acids Research*, 34(suppl_1), pp. D218–D220.

Li, P., Banjade, S., Cheng, H.-C., Kim, S., Chen, B., Guo, L., Llaguno, M., Hollingsworth, J. V., King, D. S., Banani, S. F., Russo, P. S., Jiang, Q. X., Nixon, B. T. and Rosen, M. K. (2012) 'Phase transitions in the assembly of multivalent signalling proteins', *Nature*. Nature Publishing Group, 483(7389), p. 336.

Lin, Y., Protter, D. S. W., Rosen, M. K. and Parker, R. (2015) 'Formation and maturation of phase-separated liquid droplets by RNA-binding proteins', *Molecular Cell*. Elsevier Inc., 60(2), pp. 208–219.

Magoulas, C., Zatsepina, O. V., Jordan, P. W. H., Jordan, E. G. and Fried, M. (1998) 'The SURF-6 protein is a component of the nucleolar matrix and has a high binding capacity for

nucelic acids in vitro', *EJCB*, 75(2), pp. 174–183.

Meng, F., Na, I., Kurgan, L. and Uversky, V. (2016) 'Compartmentalization and functionality of nuclear disorder : intrinsic disorder and protein-protein interactions in intra-nuclear compartments', *International Journal of Molecular Sciences*, 17(1), p. 24.

Meyers, R. M., Bryan, J. G., Mcfarland, J. M., Weir, B. A., Sizemore, A. E., Xu, H., Dharia, N. V., Montgomery, P. G., Cowley, G. S., Pantel, S., Goodale, A., Lee, Y., Ali, L. D., Jiang, G., Lubonja, R., Harrington, W. F., Strickland, M., Wu, T., Hawes, D. C., Zhivich, V. A., Wyatt, M. R., Kalani, Z., Chang, J. J., Okamoto, M., Stegmaier, K., Golub, T. R., Boehm, J. S., Vazquez, F., Root, D. E., Hahn, W. C. and Tsherniak, A. (2017) 'Computational correction of copy-number effect improves specificity of CRISPR-Cas9 essentiality screens in cancer cells', *Nat. Genet.*, 49(12), p. 1779. doi: 10.1038/ng.3984.Computational.

Miyoshi, M., Okajima, T., Matsuda, T., Fukuda, M. N. and Nadano, D. (2007) 'Bystin in human cancer cells : intracellular localization and function in ribosome biogenesis', *Biochem J.*, 404(3), pp. 373–381.

Molliex, A., Temirov, J., Lee, J., Coughlin, M., Kanagaraj, A. P., Kim, H. J., Mittag, T. and Taylor, J. P. (2015) 'Phase separation by low complexity domains promotes stress granule assembly and drives pathological fibrillization', *Cell*. Elsevier Inc., 163(1), pp. 123–133.

Mullem, V. Van, Landrieux, E., Vandenhaute, J. and Thuriaux, P. (2002) 'Rpa12p , a conserved RNA polymerase I subunit with two functional domains', *Molcular Microbiology*, 43(5), pp. 1105–1113.

Nott, T. J., Petsalaki, E., Farber, P., Jervis, D., Fussner, E., Plochowietz, A., Craggs, T. D., Bazett-Jones, D. P., Pawson, T., Forman-Kay, J. D. and Baldwin, A. J. (2015) 'Phase transition of a disordered nuage protein generates environmentally responsive membraneless organelles', *Molecular Cell*. The Authors, 57(5), pp. 936–947.

Ohta, S., Bukowski-Wills, J. C., Sanchez-Pulido, L., Alves, F. de L., Wood, L., Chen, Z. A., Platani, M., Fischer, L., Hudson, D. F., Ponting, C. P., Fukagawa, T., Earnshaw, W. C. and Rappsilber, J. (2010) 'The protein composition of mitotic chromosomes determined using multiclassifier combinatorial proteomics', *Cell*. Elsevier Ltd, 142(5), pp. 810–821.

Olson, M. O. J., Dundr, M. and Szebeni, A. (2000) 'The nucleolus: an old factory with unexpected capabilities', *Trends in cell biology*, 10(5), pp. 189–196.

Pinello, L., Canver, M. C., Hoban, M. D., Orkin, S. H., Kohn, D. B., Bauer, D. E. and Yuan, G. C. (2016) 'Analyzing CRISPR genome-editing experiments with CRISPResso', *Nature Biotechnology*, 34(7), p. 695.

Rozenblatt-Rosen, O., Hughes, C. M., Nannepaga, S. J., Shanmugam, K. S., Copeland, T. D., Guszczynski, T., Resau, J. H. and Meyerson, M. (2005) 'The parafibromin tumor suppressor protein is part of a human Paf1 complex', *Molecular and cellular biology*, 25(2), pp. 612–620.

Sasaki, T., Toh-e, A. and Kikuchi, Y. (2000) 'Yeast Krr1p physically and functionally interacts with a novel essential Kri1p , and both proteins are required for 40S ribosome biogenesis in the nucleolus', *Molecular and cellular biology*, 20(21), pp. 7971–7979.

Savino, T. M., Gébrane-Younès, J., De Mey, J., Sibarita, J.-B. and Hernandez-Verdun, D. (2001) 'Nucleolar Assembly of the rRNA Processing Machinery in Living Cells', *The Journal of Cell Biology*, 153(5), pp. 1097–1110.

Scherl, A., Couté, Y., Déon, C., Callé, A., Kindbeiter, K., Sanchez, J.-C., Greco, A., Hochstrasser, D. and Diaz, J.-J. (2002) 'Functional proteomic analysis of human nucleolus', *Molecular Biology of the Cell*, 13(11), pp. 4100–4109.

Sheval, E. V., Polzikov, M. A., Olson, M. O. J. and Zatsepina, O. V. (2005) 'A higher concentration of an antigen within the nucleolus may prevent its proper recognition by specific antibodies', *European Journal of Histochemistry*, pp. 117–124.

Sirri, V., Jourdan, N., Hernandez-Verdun, D. and Roussel, P. (2016) 'Sharing of mitotic pre-ribosomal particles between daughter cells', *Journal of Cell Science*, 129(8), pp. 1592–1604.

Stadler, C., Skogs, M., Brismar, H., Uhlén, M. and Lundberg, E. (2010) 'A single fixation protocol for proteome-wide immunofluorescence localization studies', *Journal of Proteomics*. Elsevier B.V., 73(6), pp. 1067–1078.

Svistunova, D. M., Musinova, Y. R., Polyakov, V. Y. and Sheval, E. V. (2012) 'A simple method for the immunocytochemical detection of proteins inside nuclear structures that are inaccessible to specific antibodies', *Journal of Histochemistry & Cytochemistry*, 60(2), pp. 152–158.

Takata, H., Uchiyama, S., Nakamura, N., Nakashima, S., Kobayashi, S., Sone, T., Kimura, S., Lahmers, S., Granzier, H., Labeit, S., Matsunaga, S. and Fukui, K. (2007) 'A comparative proteome analysis of human metaphase chromosomes isolated from two different cell lines reveals a set of conserved chromosome-associated proteins', *Genes to Cells*, 12(3), pp. 269–284.

The UniProt Consortium (2019) 'UniProt: a worldwide hub of protein knowledge', *Nucleic Acids Research*, 47(D1), pp. D506–D515.

Thul, P. J., Åkesson, L., Wiking, M., Mahdessian, D., Geladaki, A., Ait Blal, H., Alm, T., Asplund, A., Björk, L., Breckels, L. M., Bäckström, A., Danielsson, F., Fagerberg, L., Fall, J., Gatto, L., Gnann, C., Hober, S., Hjelmare, M., Johansson, F., Lee, S., Lindskog, C., Mulder, J., Mulvey, C. M., Nilsson, P., Oksvold, P., Rockberg, J., Schutten, R., Schwenk, J. M., Sivertsson, Å., Sjöstedt, E., Skogs, M., Stadler, C., Sullivan, D. P., Tegel, H., Winsnes, C., Zhang, C., Zwahlen, M., Mardinoglu, A., Pontén, F., von Feilitzen, K., Lilley, K. S., Uhlén, M. and Lundberg, E. (2017) 'A subcellular map of the human proteome', *Science*, 356(6340), p. eaal3321.

Uhlen, M., Bandrowski, A., Carr, S., Edwards, A., Ellenberg, J., Lundberg, E., Rimm, D. L., Rodriguez, H., Hiltke, T., Snyder, M. and Yamamoto, T. (2016) 'A proposal for validation of antibodies', *Nature methods*, 13(10), p. 823.

Uhlen, M., Oksvold, P., Fagerberg, L., Lundberg, E., Jonasson, K., Forsberg, M., Zwahlen, M., Kampf, C., Wester, K., Hober, S., Wernerus, H., Björling, L. and Ponten, F. (2010) 'Towards a knowledge-based Human Protein Atlas.', *Nature biotechnology*, 28(12), p. 1248.

Uhlen, M., Zhang, C., Lee, S., Sjöstedt, E., Fagerberg, L., Bidkhori, G., Benfeitas, R., Arif, M., Liu, Z., Edfors, F., Sanli, K., von Feilitzen, K., Oksvold, P., Lundberg, E., Hober, S., Nilsson, P., Mattsson, J., Schwenk, J. M., Brunnström, H., Glimelius, B., Sjöblom, T., Edqvist, P.-H.,

Djureinovic, D., Micke, P., Lindskog, C., Mardinoglu, A. and Ponten, F. (2017) 'A pathology atlas of the human cancer transcriptome', *Science*, 357(6352), p. eaan2507.

Uversky, V. N., Oldfield, C. J. and Dunker, A. K. (2008) 'Intrinsically disordered proteins in human diseases : introducing the D2 concept', *Annu. Rev. Biophys.*, 37, pp. 215–246.

Visintin, R. and Amon, A. (2000) 'The nucleolus : the magician ' s hat for cell cycle tricks', *Current Opinion in Cell Biology*, 12(3), pp. 372–377.

Weisenberger, D. and Scheer, U. (1995) 'A possible mechanism for the inhibition of ribosomal RNA gene transcription during mitosis', *The Journal of Cell Biology*, 129(3), pp. 561–575.

Westendorf, J. M., Konstantinov, K. N., Wormsley, S., Shu, M.-D., Matsumoto-taniura, N., Pirollet, F., Klier, F. G., Gerace, L. and Baserga, S. J. (1998) 'M phase phosphoprotein 10 is a human U3 small nucleolar ribonucleoprotein component', *Molecular Biology of the Cell*, 9(2), pp. 437–449.

Zhao, L., Tong, T. and Zhang, Z. (2005) 'Expression of the Leo1-like domain of replicative senescence down-regulated Leo1-like (RDL) protein promotes senescence of 2BS fibroblasts', *The FASEB journal*, 19(6), pp. 521–532.